VYSOKÉ UČENÍ TECHNICKÉ V BRNĚ
BRNO UNIVERSITY OF TECHNOLOGY

FAKULTA CHEMICKÁ
ÚSTAV CHEMIE MATERIÁLŮ

FACULTY OF CHEMISTRY
INSTITUTE OF MATERIALS SCIENCE

FUNCTIONALIZATION OF POLY(LACTIC ACID)

DIZERTAČNÍ PRÁCE
DOCTORAL THESIS

AUTOR PRÁCE Ing. JOSEF PETRUŠ
AUTHOR

BRNO 2015

VYSOKÉ UČENÍ TECHNICKÉ V BRNĚ

BRNO UNIVERSITY OF TECHNOLOGY

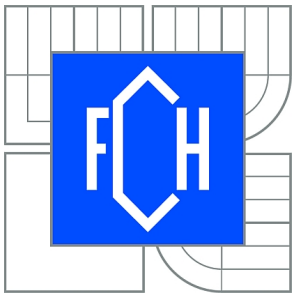

FAKULTA CHEMICKÁ
ÚSTAV CHEMIE MATERIÁLŮ

FACULTY OF CHEMISTRY
INSTITUTE OF MATERIALS SCIENCE

FUNCTIONALIZATION OF POLY(LACTIC ACID)

FUNKCIONALIZACE POLY(MLÉČNÉ KYSELINY)

DIZERTAČNÍ PRÁCE
DOCTORAL THESIS

AUTOR PRÁCE — Ing. JOSEF PETRUŠ
AUTHOR

VEDOUCÍ PRÁCE — doc. RNDr. JAROSLAV PETRŮJ, CSc.
SUPERVISOR

BRNO 2015

Vysoké učení technické v Brně
Fakulta chemická
Purkyňova 464/118, 61200 Brno 12

Zadání dizertační práce

Číslo dizertační práce:	**FCH-DIZ0115/2015**	Akademický rok: **2015/2016**
Ústav:	Ústav chemie materiálů	
Student(ka):	**Ing. Josef Petruš**	
Studijní program:	Makromolekulární chemie (P1422)	
Studijní obor:	Chemie makromolekulárních materiálů (1405V003)	
Vedoucí práce	**doc. RNDr. Jaroslav Petrůj, CSc.**	
Konzultanti:		

Název dizertační práce:

Funkcionalizace poly(mléčné kyseliny)

Zadání dizertační práce:

Cílem disertační práce je příprava a charakterizace poly(mléčné kyseliny) PLA roubované pomocí anhydridu kyseliny itakonové IAH na kopolymer (PLA-g-IAH).

Termín odevzdání dizertační práce: 30.10.2015

Dizertační práce se odevzdává v děkanem stanoveném počtu exemplářů na sekretariát ústavu a v elektronické formě vedoucímu dizertační práce. Toto zadání je přílohou dizertační práce.

Ing. Josef Petruš Student(ka)	doc. RNDr. Jaroslav Petrůj, CSc. Vedoucí práce	prof. RNDr. Josef Jančář, CSc. Ředitel ústavu

V Brně, dne 1.9.2015

prof. Ing. Jaromír Havlica, DrSc.
Děkan fakulty

ABSTRACT

The theoretical part of proposed thesis describes principle of radical grafting as well as the most important controlling factors affecting reaction course. Radical grafting of poly(lactic acid) (PLA) via reactive modification is the most promising technique for the preparation of biodegradable polymeric materials with various properties. Actual knowledge of PLA modification via radical grafting in melt is mentioned in the literature review as well as its potential applications.

Experimental part deals with functionalization of PLA with itaconic anhydride (IAH) via radical grafting in the melt. Grafting reaction was initiated by 2,5-bis(tert-butylperoxy)-2,5-dimethylhexane (L101).

In the first part, radical grafting is investigated "in situ" using differential scanning calorimetry (DSC) and thermogravimetric analysis (TGA). Exothermic peak on DSC thermogram reflects grafting reaction which allows calculation of activation energy of reaction. With regard to "in situ" TGA thermogram, formation of byproducts during radical modification was observed.

In the second part, functionalization of PLA was achieved in discontinuous internal mixer under defined reaction conditions which were tailored to half-life time of chosen initiator and PLA processing parameters. Reaction temperature 190 °C was calculated according to Arrhenius equation and reaction time 6 min. These conditions were considered to be convenient with respect to decomposition kinetics of L101 and suppression of PLA degradation. IAH was succesfully grafted onto PLA backbone which was proved by Fourier transform infrared spectroscopy (FTIR) due to presence of $-CH_2$ vibrations at 2860 and 2920 cm^{-1}. Increase of integral intensity of the absorption band centered at 1750 cm^{-1} proved appearance of anhydride C=O vibrations overlapped by C=O vibrations of PLA backbone. Nuclear magnetic resonance (^{1}H-NMR) did not detect oligomeric IAH grafted onto PLA. Different concentration of reactants (0.5–10 wt % of IAH, 0.1–2 wt % of L101) was applied in order to evaluate its influence on grafting yield and the extent of side reactions such as β-scission, branching and crosslinking. At high concentration of both IAH and L101, IAH homopolymerization occurs although it is neglected in the most of research works. This argument is supported by colorimetric analysis, characterization of samples prepared by polymerization of IAH under grafting conditions and thermal stability of fractions extracted from PLA-g-IAH. Radical modification of PLA improves chain flexibility due to bulky IAH which was detected as a decrease of glass transition temperature (T_g). Increased content of amorphous phase, improved hydrophilicity, branched structure and chain scission enhanced biodegradability of PLA-g-IAH compared to neat PLA.

Non-radical degradation during processing was proved by change of melt behaviour. This undesired effect was suppressed by addition of chain extender with reactive epoxy groups. Reaction between epoxy groups of chain extender and carboxyl groups of PLA was proved by structure analysis and change of rheological behavior of PLA-g-IAH.

KEYWORDS

Radical grafting, poly(lactic acid), itaconic anhydride, homopolymerization.

ABSTRAKT

Teoretická část předložené dizertační práce popisuje princip radikálového roubování a faktory ovlivňující reakční průběh. Radikálové roubování poly(mléčné kyseliny) (PLA) reaktivní modifikací je vhodnou technikou přípravy biodegradabilních polymerních materiálů s rozličnými vlastnostmi. Současný stav problematiky modifikace poly(mléčné kyseliny) radikálovým roubováním v tavenině je obsahem literární rešerše včetně možných aplikací.

Experimentální část se zabývá modifikací PLA anhydridem kyseliny itakonové (IAH) radikálovým roubováním v tavenině. Reakce byla iniciována 2,5-bis(tert-butylperoxy)-2,5-dimethylhexanem (L101).

V první části je průběh radikálového roubování pozorován "in situ" pomocí diferenciální kompenzační kalorimetrie (DSC) a termogravimetrické analýzy (TGA). Exotermní pík na DSC záznamu odpovídá průběhu radikálové reakce, na jehož základě lze definovat aktivační energii reakce. Průběh TGA křivky "in situ" radikálové reakce umožnil detekovat vedlejší produkty vznikající v průběhu radikálové modifikace.

Ve druhé části byla PLA funkcionalizována reakcí v diskontinuálním laboratorním mixéru za reakčních podmínek navržených dle poločasu rozpadu zvoleného iniciátoru a zpracovatelských podmínek PLA. Reakční teplota 190 °C byla stanovena výpočtem z Arrheniovy rovnice pro reakční čas 6 min. Uvedené reakční parametry byly zvoleny s ohledem na kinetiku rozkladu L101 a potlačení degradace PLA. Infračervená spektroskopie (FTIR) potvrdila navázání IAH na PLA řetězec na základě výskytu $-CH_2$ vibrací s absorpčními pásy při vlnočtu 2860 a 2920 cm^{-1}. Vzrůstající intensita absorpčního pásu 1750 cm^{-1} potvrdila přítomnost minoritních C=O vibrací anhydridového kruhu překrytých dominantními C=O vibracemi PLA řetězce. Nukleární magnetická rezonance (^{1}H-NMR) nepotvrdila roubování oligomerního IAH na PLA. Koncentrace reaktantů ve zvoleném rozsahu (0.5–10 hm % IAH, 0.1–2 hm % L101) byla použita pro posouzení jejího vlivu na obsah naroubovaného IAH a míru vedlejších reakcí, např. β-štěpení, větvení a síťování. Při vysoké koncentraci IAH a L101 byla potvrzena homopolymerace IAH i přes její zanedbávání v tématicky podobných studiích. Tvrzení o IAH homopolymeraci bylo podpořena výsledky kolorimetrické analýzy, charakterizací vzorků připravených polymerací IAH za podmínek radikálového roubování a termickou stabilitou frakcí extrahovaných z PLA-g-IAH. Radikálovou modifikací PLA došlo ke zvýšení flexibility polymerních řetězců díky objemné struktuře IAH navázané na PLA řetězci, což se projevilo poklesem teploty skelného přechodu (T_g). Zvýšený obsah amorfní fáze, hydrofilní chování, rozvětvená struktura a štěpení řetězců má pozitivní vliv na zvýšenou biodegradabilitu PLA-g-IAH v porovnání s nemodifikovanou PLA.

Neradikálová degradace, probíhající v průběhu zpracování PLA, byla prokázána změnou tokových vlastností taveniny. Tento nežádoucí jev byl potlačen přídavkem tzv. "prodlužovače řetězců" obsahujícího reaktivní epoxy skupiny. Reakce mezi epoxy skupinami a karboxylovými skupinami byla potvrzena pomocí FTIR a změnou reologických vlastností PLA-g-IAH.

KLÍČOVÁ SLOVA

Radikálové roubování, poly(mléčná kyselina), anhydrid kyseliny itakonové, homopolymerace.

PETRUŠ, J. Funkctionalization of poly(lactic acid). Brno: Brno University of Technology, Faculty of Chemistry, 2015. 66 p. Supervisor doc. RNDr. Jaroslav Petrůj, CSc.

Declaration

I declare that the doctoral thesis has been worked out by myself and that all the quotations from the used literary sources are accurate and complete.

.....
student's signature

Acknowledgements

I would like to thank my supervisor doc. RNDr. Jaroslav Petrůj, CSc. for his professional guidance and prof. RNDr. Josef Jančář, CSc. for providing me the working conditions. I would also like to thank Mgr. František Kučera for discussions and consulting, Dr. Robert A. Weiss for the oportunity to pass the research fellowship at the University of Akron, Department of Polymer Engineering, U.S. and Ing. Radka Bálková, Ph.D. for discussions regarding thermal analysis.
Finally, I would like to thank my dear wife Pavlínka for her endless love and support, my parents for providing me convenient conditions and also all my colleagues, at Faculty of Chemistry, BUT, at the Department of Materials Science, for their help.

TABLE OF CONTENTS

1. INTRODUCTION

Polymer industry in the Czech Republic is focused especially on processing of petroleum-based polymers, such as polyolefins. This situation is given by history of industry in the Czech Republic and relatively low interest in polymer recyclation. Processing of poly(lactic acid) and its modification could lead to higher interest in biodegradable and recyclable polymers with higher applicability in modern applications.

Modification of polymers via reactor and post-polymerization techniques is one of the most promising methods how to prepare new functional materials. Reactor methods are based on the polymer modification via polymerization (e.g. copolymerization). On the other hand, post-polymerization techniques provide new materials via processing of commercially available polymers where no preparation of new monomer is required (e.g. blending, grafting).

Importance of post-polymerization modifications arises from requirement of wider applicability of polymers and for tailoring. For example, post-polymerization modification of PLA promises to improve miscibility with different thermoplastics to enhance poor mechanical properties. Moreover, improved miscibility with certain thermoplastic may lead to substitution of hardly recyclable thermoplastics with biodegradable PLA. Experiences from the modification of commonly used polymers can be applied for modification of PLA. This fact makes PLA more attractive.

Theoretical part of this work is focused on the description of radical grafting as commonly used post-polymerization modification method. One of the first applications of radical grafting was an effort to increase polarity of nonpolar polymers due to grafting of polar monomers onto polymer backbone. Thus modified polymers exhibited enhanced miscibility with polar polymers. For example, polypropylene grafted with maleic anhydride via reactive extrusion allowed to prepare polymer blends with polyamides with improved morphology and mechanical properties compared to unmodified polypropylene used for blending.

Recently, polymer modifications are applied for large scale of polymers including PLA which is interesting for its biodegradability, recyclability and specific properties. PLA can be obtained from renewable resources and has potential to replace traditional polymers in specific applications. PLA biodegradability is desired in applications where life cycle of products is controlled. However, thermal and hydrolytical degradation requires defined condition upon processing cycle and limits processing at elevated temperatures. Reactor modification of PLA with epoxy compounds or unsaturated compounds gives polymers which are coupled via radical reaction with elastomers [1]. PLA grafted with suitable monomer by post-polymerization modification may be used as a compatibilizer in polymer blends and composites which reduce interphase tension leading to enhanced adhesion to polymer matrix or filler [2]. Finally, biodegradability and other properties can be combined in resulting material.

2. THEORETICAL PART

2.1 Principle of polymer modification via radical grafting

Radical grafting is used to modification of polymers via reaction with monomer(or monomers) is bonded onto polymer chain. One monomer is usually grafted within one-step reaction. Two or more monomers can be grafted simultaneously or in sequence reaction steps. Bonding of new functional groups via grafting reaction affects hydrophility, solubility, thermal properties or adhesion. Scheme of radical grafting is illustrated for radical grafting of biomacromolecule with appropriate monomer in Figure 1. It can be noted that proposed scheme can be generalized for any polymeric material. Three general grafting methods can be distinguished: a) Grafting to: A pre-existing polymer with a functional chain end-group reacts with a complementary functional group present on the biomacromolecule; thus prepared grafted or crosslinked polymers prepared using crosslinking agent; b) Grafting from: Polymerization originates from a specific site on the biomacromolecule that is capable of producing radicals (e.g. initiator) and initiates polymerization of monomer; c) Grafting through: Radical polymerization occurs in the presence of a biomacromolecule that contains a polymerizable group, thus acting as a monomer, and can copolymerize with a different type of monomer to yield a polymeric chain bearing biomacromolecules attached to its backbone [3].

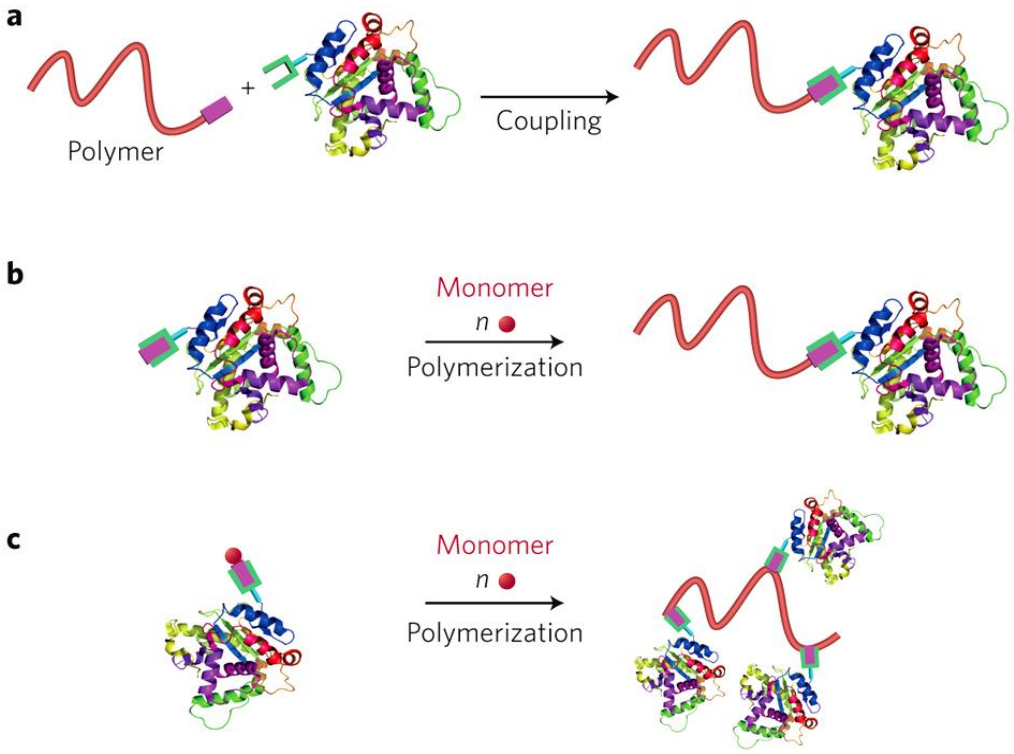

Figure 1. Scheme of radical grafting methods; grafting to (a), grafting to (b) and grafting through (c) [4].

Depending on the reaction conditions, grafting reaction may run according to different mechanisms – direct or indirect, chemical or physical. Based on the initiation process, grafting methods can be sorted on chemical, photochemical, enzymatic, radiation and plasma-induced grafting [3].

In the grafting reaction, formation of reactive species (radicals, ions) is the key step for bonding of monomer onto polymer backbone or covalent bonding of two polymer chains (see Figure 1). Regarding grafting method applied in experimental part of this work, free-radical grafting is the most commented method below. Primary radicals can be generated via chemical reaction (i.e. redox reaction), by application of energy needed for homolytical scission of C–H, O–O or C–C bond or application of radiation for generation of excited species (UV, plasma, photochemical decomposition, etc.). Most cited ways are schemed in Figure 2 [5].

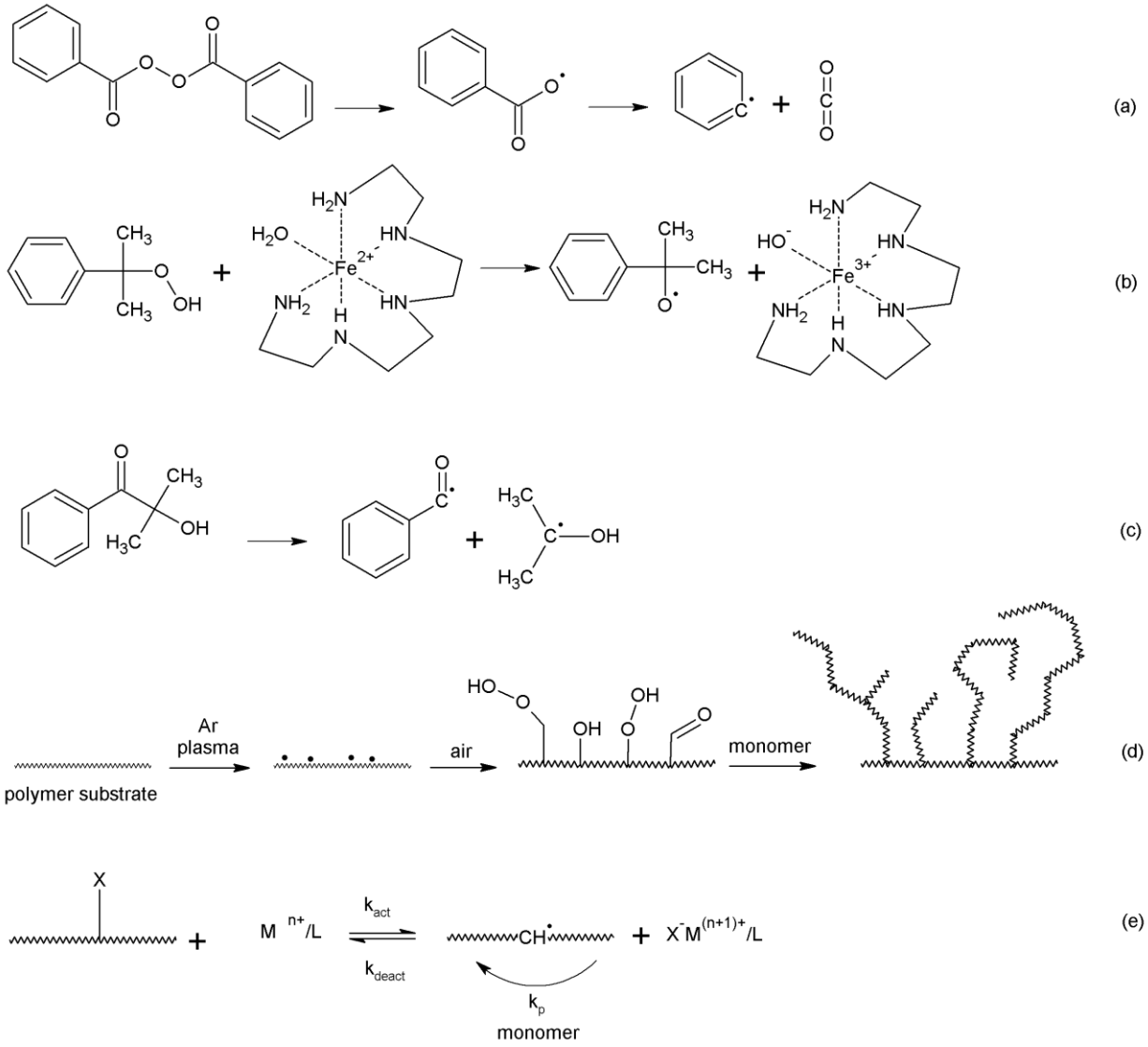

Figure 2. Radical grafting initiated by: DBP decomposition (a); formation of cumyl radicals by redox reaction (b); photochemical decomposition of photoinitiator (2-hydroxy-2-methyl-1-fenylpropan-1-on) (c); plasma (d); living radical formation through atom transfer (e) [5].

2.2 Radical grafting initiated by decomposition of thermolabile compounds

Chemically initiated radical grafting can be realized according to mechanisms depicted in Figure 2. Different types of initiators affect course of reaction as well as mechanism of primary radicals generation. Most common mechanisms include decomposition of thermolabile compounds, redox reactions and other specific reactions, such as enzymatic reactions or atom transfer reaction.

Most of grafting methods are based on the radical reactions in melt. Compared to other grafting methods, reactions in melt can be achieved under different reaction conditions using different industrial devices (i.e. extruders, mixers, kneaders) providing high efficiency of polymer modification. Peroxides, hydroperoxides and azocompounds are commonly used for generation free radicals. Free radicals attack polymer chain and thus formed active center can react with monomer [6]–[8]. Table 1 summarizes compounds with peroxide bond R–O–O–R' which is homolytically decomposed onto highly reactive primary radicals containing unpaired electron in their structure. Initiators can be sorted acoording to ability to form active center on polymer chain and half-life time $\tau_{1/2}$ affecting reaction conditions (e.g. temperature, time). An overview of commonly used initiators as well as relating $\tau_{1/2}$ summarized Table 1.

Table 1. Overview of commonly used thermal initiators [9].

Structure, name, abbreviation	**T [°C] = $f(\tau_{1/2})$**		
	10 h	**1 h**	**0,1 h**
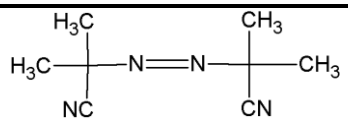 2,2′-azodi(isobutyronitril) (AIBN)	64	82	101
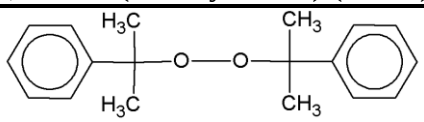 Dicumyl peroxide (DCP)	116	136	175
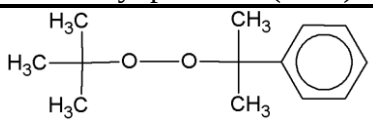 t-butyl α-cumyl peroxide (BCP)	118	138	180
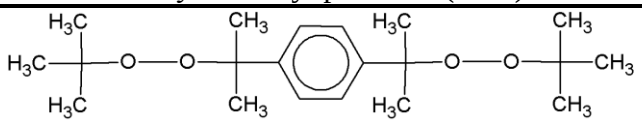 α,α′-di(t-butyl-peroxy)-1,3-diisopropyl benzen (DBPIB)	120	142	190
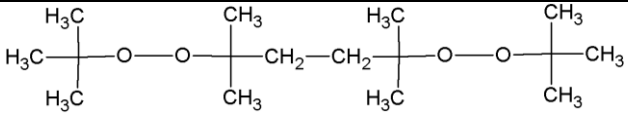 2,5-di(t-butyl-peroxy)-2,5-dimethyl hexane (DTBPH)	120	142	190

Overall scheme of free-radical grafting onto polymer backbone presentes by Al-Malaika [9] usually contains three types of reactants: polymer, unsaturated monomer and free radical initiator. Primary radicals are generated in the presece of polymer and monomer by specific decomposition mechanism depending on the type of initiator. Regarding scheme in Figure 3, primary radicals can participate on two different reactions with monomer - homopolymerization and grafting. Homopolymerization occurs upon reaction between free radical and monomer whereas further addition of monomer results in formation of oligomers and polymers (reaction b). Grafting starts with hydrogen atom abstraction which was described above. Grafting of oligomeric chain is less probable due to limited hydrogen atom abstraction. After hydrogen atom abstraction (reaction a), three different reactions may be observed. Except of desired reaction between macroradical and monomer (reaction a3), chain scission (reaction a1) or crosslinking (reaction a2) can be observed. Macroradical of grafted monomer can act as a center suitable for bonding new monomer molecules, extending of grafted chain (reaction a3-1) or hydrogen atom transfer (reaction a3-2) [9].

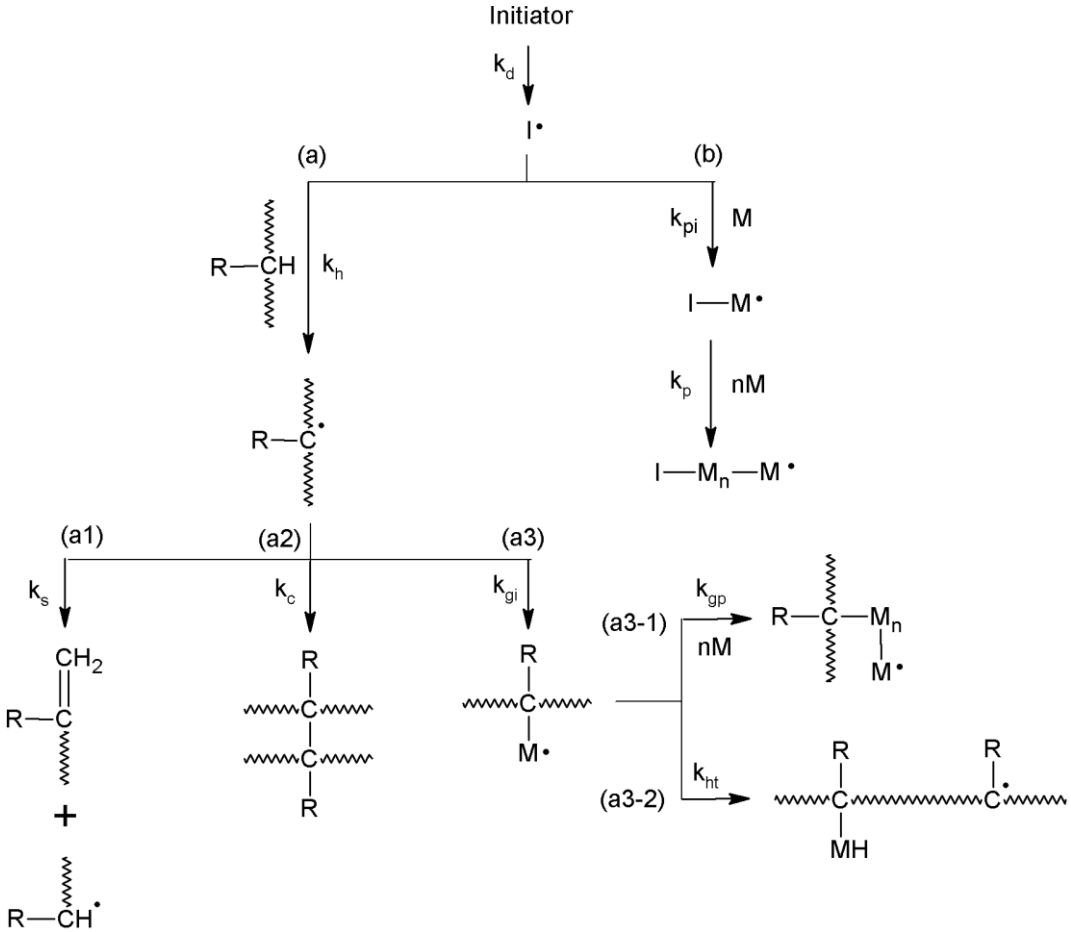

Figure 3. Mechanism of: homopolymerization of monomer (b), hydrogen atom abstraction (a) with subsequent β-scission (a1); crosslinking (a2) and monomer grafting (a3]; homopolymerization of grafted monomer (a3-2) and intramolecular transfer of hydrogen atom forming new active center (a3-1) [9].

2.2.1 Mechanism of radical grafting

Initiation

Initiation is the particalr reaction controlling the kinetics of grafted polymers prepared by a radical mechanism. Initiation can be divided into three parts:

1) Generation of the initial radical species.
2) Reaction of these species to generate other radicals.
3) Addition of either the initial radical, or its products, to a monomer, to begin the propagation reactions.

Equations 1a–c represent simplified scheme of free radicals generation via thermal decomposition and subsequent steps included in initiating part. Thermal decomposition of initiator is given by Equation 1a. Equation 1b represents homopolymerization of monomer due to reaction between primary radical and monomer unit. Substitution reaction between primary radicals and polymer results in hydrogen atom abstraction where macroradical is formed (Equation 1c) [5].

$$I_2 \longrightarrow 2\,I\cdot \tag{1a}$$

$$I\cdot + M \rightarrow IM\cdot \xrightarrow{+M} IMM\cdot \tag{1b}$$

$$I\cdot + RH \longrightarrow R\cdot + IH \tag{1c}$$

Generation of the initial radicals depends predominately on the nature of the initiator. Radical grafting can be controlled by by choice of sufficient initiator with low volatility of decomposition products, toxicity, susceptible $\tau_{1/2}$ and high initiating efficiency [5], [10], [11]. For a given chemical initiator the dissociation rate can be controlled by varying the temperature and a wide range of radical fluxes can be generally achieved by varying the initiator concentration. The extent of subsequent reactions of radical species depends on other reactants presented in the reaction system such as polymer substrate, monomer, additives, etc.

As mentiond in previous chapter, dialkyl peroxides are commonly used for initiation of radical grafting. In the most cases, an initiator is initially homogeneously distributed which is typical for most single-phase reactions using a peroxy initiators as mentioned above. The rate of gthus generated free radicals $I^{\bullet}$ is the same everywhere in the system and can be given by Equation 2:

$$-\frac{d\left[I^{\bullet}\right]}{dt} = f\cdot k_d\cdot\left[I\right] \tag{2}$$

where [I] is a function of time, k_d is rate coefficent which can be considered to include the stoichiometry of the decomposition and f represents viscosity-dependent constant which includes “cage effect” where two radicals held in close proximity combine to form an unreactive

product. Constant *f* determines the effectivity of flux of radicals. Because of high viscosity of reaction system, decrease of [I$^{\bullet}$] due to recombination reactions will be large and *f* will be small. It is in contrast with grafting in dilute solution which exhibit much higher effectivity of radical flux compared to grafting in high viscous system.

Generally, peroxide initiators can be distinguished regarding their decomposition products. For example, thermal decomposition of cumylhydroperoxide gives cumyloxy radicals (Figure 4, reaction a) whereas, for example, dibenzoylperoxide provides benzoxy radicals with subsequent scission onto secondary phenyl radicals. The decomposition mechanism of dialkyl peroxides is well established as involving initial O–O bond homolysis to generate the corresponding alkoxy radicals. If not trapped by reaction with substrate, the initially formed alkoxy radicals undergo *β*-scission with preferential cleavage of the weakest C–C bond. Bonds to sp^3 carbons are broken rather than bonds to sp (acetylenic) or sp^2 (aromatic, olefinic) carbons. Bonds to higher alkyl chains are cleaved in preference to those to methyl radicals.

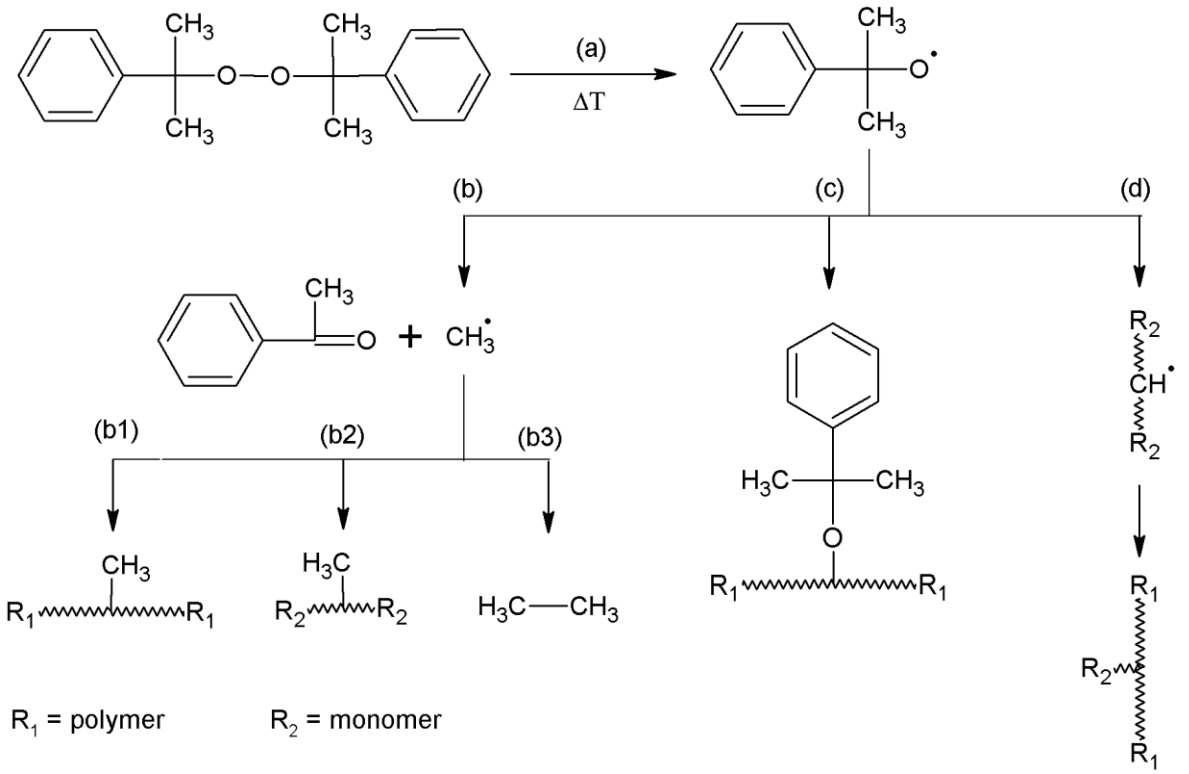

Figure 4. Homolytical decomposition of dicumyl peroxide (a); β-scission of cumyloxy radicals to secondary methyl radicals (b); addition of secondary methyl radicals on polymer (b1), monomer (b2) and recombination (b3); addition of primary cumyloxy radicals on polymer chain (c); hydrogen atom abstraction from molecule of monomer using cumyloxy primary radicals with subsequent addition of monomer onto polymer (d) [12].

Detailed description of dicumylperoxide decomposition within grafting of surface nanotubes with pentadecane was proposed by Akbar et al. [12]. Authors concluded that higher temperatures resulted in higher amount of secondary methyl radicals $CH_3^{\bullet}$ due to thermal decomposition of

dicumylperoxide with subsequent β-scission of cumyloxy radicals. In the next step, methyl radicals recombined (Figure 4, reaction b3) or were bonded to either polymer and/or monomer (Figure 4, reaction b1 and b2). Second reaction way occured due to reaction conditions which prefer formation of cumyloxy radicals which abstract hydrogen atom from pentadecane or radical is bonded onto polymer chain (Figure 4, reaction c). Cumyloxy radicals can be also decomposed to phenyl radicals and acetone as a byproduct. Both phenyl and methyl radicals are nonselective against C–H bonds due to high strength of C–H bond included in benzene ring and methane. Different reactivity of primary and secondary radicals allows control of reaction course.

Radicals formed via thermal decomposition of peroxide initiators may undergo two different reaction types leading to formation of initiating species - abstraction and addition. It is well established that the reactivity and specificity shown by initiator-derived radicals in abstraction and addition reactions depend strongly on the nature of the radicals and thus on the particular initiator. Abstraction is an efficient way for O–O bond containing initiators to introduce a reactive center to the backbone or side chain of a polymer [5]. This kind of reactions depends on the hydrogen-abstracting capacity of the radical and susceptibility of the substrate to abstraction. In the case of hydrogen-abstracting capacity, heteroatom-centered radicals are usually considered to be more effective in abstraction on electronic grounds, and a relatively persistent radical will usually be more reactive toward abstraction than addition on steric grounds. Abstraction efficiency is also given by the strenght of R–X in polymer substrate which is needed for removing $X^{\bullet}$ while $R^{\bullet}$ is formed. Table 2 summarizes dissociation energies of different C–H bonds including activation energies which are necessary for hydrogen atom abstraction. Typical values of activation energies of abstraction relevant to grafting are of the order 20–30 $kJ \cdot mol^{-1}$ [13].

Table 2. Disociation energies E_d of C–H bond needed for hydrogen abstraction depending on the kind of carbon atom [14].

Bond	E_d **(C–H) [kJ/mol]**	**Bond**	E_d **(C–H) [kJ/mol]**	**Bond**	E_d **(C–H) [kJ/mol]**
$(R_3)C–H$	404	$C_2H_5O–H$	435	$C_2H_5–H$	410
$(R_2)CH–H$	413	$CH_3–H$	435	$C_3H_7–H$	395
$RCH_2–H$	423	Phenyl–H	463	$C_4H_9–H$	384

Addition mechanism is based on replacement of high energy π-bond by σ-bond. Weak C–H bond of tertiary carbon (E_d = 404 $kJ \cdot mol^{-1}$) is replaced by stronger O–H bond formed via reaction between hydrogen atom and peroxide radical $R–O^{\bullet}$ (E_d = 463 $kJ \cdot mol^{-1}$) [8]. Addition mechanism is typical for radicals with C–C bond [5]. The addition to a double bond in the polymer is a common means for a small radical to generate a reactive center [15]. Common polymers based on a diene monomer, such as polyisoprene and polybutadiene, have both double bonds in the backbone and pendant double bonds to which addition may take place.

In radical grafting, the final step of initiation will be when the radical center R$^{\bullet}$ adds to a molecule of a monomer. If R$^{\bullet}$ is localized on the polymer backbone, this will give the "grafting from" process; if R$^{\bullet}$ is a small molecule, this will give a potential "grafting to" process. This step is unlikely to be rate-controlling unless the previous steps of initiation give rise to persistent radicals.

Propagation

Propagation is the next step subsequent to initiation. It consists of a large number of reactions which occur once initiation is complete and all events occurring before termination form part of the "kinetic chain". These reactions may include addition to the monomer and functionalities on the polymer, or chain transfer, typically to polymer or an additive. Propagation is the key reaction determining overall kinetics of radical grafting. It can be simplified that total polymerization enthalpy equals to enthalpy of propagation. As consumption of monomer is the primary reaction, propagation ratre can be defined by Equation 3:

$$-\frac{d[M]}{dt} = k_p \cdot [\Sigma R^{\bullet}] \cdot [M] \qquad (3)$$

where $\Sigma R^{\bullet}$ is the sum of all radical species that can interact withmonomer. As [M] is initially fixed and can only decrease in the course of the reaction, [$\Sigma R^{\bullet}$] will be the main parameter controlling the kinetics. This assumes all R$^{\bullet}$ have the same reactivity, an assumption valid at degrees of polymerization greater than 10 in circumstances where there are few side reactions generating persistent radicals. If one or more comonomers are present, the rate coefficients for each of the possible propagation reactions and the possible change of the relative amounts of the comonomers over time must be considered. Monomers that are reluctant to homopolymerization, such as maleic acid or crotonic acid, generate very short grafts. As discussed previously, high viscosity limits effect of chemical control of propagation whereas physical constraints predominate.In that case propagation is controlled by the reactive diffusion of monomer to polymer radicals, giving a greatly reduced k_p value. It can be simplified that total polymerization enthalpy equals to enthalpy of propagation.

Termination

Active center can be perished in several ways which are generally based on the pairing of two radicals to form nonradical species. As this reaction is essentially barrier-less, termination is rapid and effectively diffusion controlled under all conditions. One of the most common way is reaction with relatively labile hydrogen atom with subsequent radical transfer to another polymer chain (Figure 5a). Grafting reaction can be terminated either by reaction with radical located on low-molecular oligomer (Figure 5b). Termination can occur as a result of reaction with macroradical which leads to grafting or crosslinking between two polymer chains (Figure 5c).

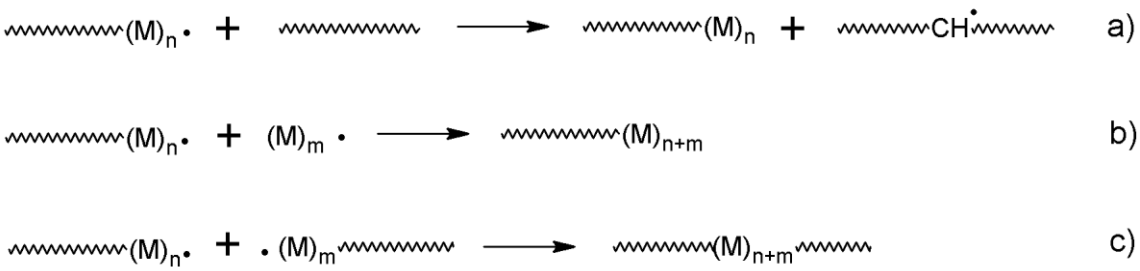

Figure 5. Termination of growing active center by a) radical transfer, b) addition of oligomeric radcial, c) interaction between two active centers.

Since the polymer radicals are much larger than the monomer, with increasing viscosity k_t decreases before k_p begins to decrease. This is the physical basis for the rapid increase in the rate of radical polymerization with viscosity over the course of a reaction [13]. An important consequence of the diffusion dependence of k_t for grafting reactions is that termination will most frequently occur not by the meeting of two large radical species but by the addition of a small mobile radical to a polymer - centered radical. "Grafting to" mechanisms will thus be unlikely except for reactions carried out in dilute solution.

Depending on chain lenght, semiempirical expressions for the chain-length dependence of k_t have been determined and these expressions are given in Table 3.

Table 3. Semiempirical expressions for the chain-length dependence of k_t.

Termination between	**Lenght dependence of k_t**	**Parameters**	**Reference**
equal and relatively short chains	$k_t^{i,i} = k_t^{1,1} \cdot i^{-es}$	s = 1/2	[16]
equal and relatively long chains	$k_t^{i,i} = k_t^{1,1} \cdot (i_{crit})^{-(es-eL)} \cdot i^{-eL}$	s = 1/2 L = 1/6	[17]
relatively short chains and polymer radicals	$k_t^{i,long} = 4 \cdot \pi \cdot D_i \cdot p_i \cdot \sigma \cdot N_A$ $D_i = c_2 \cdot D_1(x) \cdot i^{c_0 + c_1(x)}$	D_i...relative diffusion coefficient p_i...probability of radical termination σ...distance of the order of an atomic diameter x...mass fraction of polymer $D_1(x)$...diffusion coefficient of the monomer	[18]

When polymer chain with functional groups is bonded onto another polymer chain with functional groups, crosslinking occurs due to elimination or addition of low bulky radical species. In this case, crosslinking predominates over the formation of graft copolymers. Since termination is controlled by diffusion, rate coefficient of termination k_t is not a constant because of inverse relationship between k_t and lenght of the polymer chain [9].

Reactions between radicals and nonradical species require some amount of activation energy. On the other hand, radical-radical interactions are characterized by low activation energy which may complicate initiation due to radical recombination and decreases concentration of primary radicals. Due to low activation energy, the extent of radical-radical reaction is controlled by diffusion and dimension of radicals. Low-bulky radicals interact with higher probability which decreases grafting efficiency. On the other hand, bulky radicals prefer interactions with polymer chain due to slower diffusion.

2.3 State of the art of PLA functionalization

PLA relates to the class of biodegradable, thermoplastic and aliphatic polyesters which are derived from renewable resources such as corn starch or sugar cane [19]. PLA has been used in many applications such as medical implants, sutures or drug delivery systems. Introducing new functional groups onto PLA backbone paves the way to prepare composites, laminates, coated items and blend with improved properties and cost effectiveness. Functionalizing matrix polymer and the fiber/filler with highly reactive groups is perhaps the most successful strategy leading to a variety of commercial composites and alloys made by reactive processing. Possibility of chemical degradation makes PLA interesting alternative to petroleum-based polymers with tough recyclation.

Many grafting techniques can be used for production of variety functional groups onto the surface of natural polymers. Commonly used methods are melt grafting, solid state grafting, solution grafting and suspension grafting in aqueous or organic solvents. The post-polymerization free-radical functionalization process, generally performed in the melt by using extruders or melt mixers, is considered to be one of the most practical, cost effective and also green approach, since it is a solvent-free method. Regarding mentioned advantages, it can be applied for large-scale production. Functional groups such as isocyanata, amine, anhydride, carboxylic acid, epoxide and oxazoline are often introduced during reactive extrusion with a short residence time. Coupling reactions between mentioned functional groups provide interfacial bondings in composites, laminates, coated items and in immiscible polymer blends with improved control of the phase size and strong interfacial adhesion.

MAH was first monomer used for grafting onto biodegradable polymers such as poly(caprolactone), poly(butylene succinate-co-adipate) and PLA [20]–[24]. Maleation reaction mechanism has been already proposed by many authors as a complex process consisting of three steps (Figure 6). In first step, free radicals are formed via thermal decomposition of convenient initiator. In the second step, free radicals attack most labile C–H bond on backbone while PLA macroradical are generated. Finally, PLA macroradicals may react with the MAH. Radical functionalization with MAH initiated by peroxide is a complex process affected by polymer

nature and by the feed ratio between the reagents. Moreover, many concurrent side reactions can limit the grafting yield and change the polymer structure.

Many studies deal with relationship between reaction parameters and grafting degree. For example, Ramkumar, Bhattacharya and Vaidya [22] mentioned increase of grafting degree with increase of concentration of initiator. Same results were presented by Carlson et al. [21] who performed free-radical-initiated grafting of MAH onto a PLA backbone at 180–200 °C initiated by 2,5-dimethyl-2,5-di-(tert-butylperoxy) hexane (Lupersol 101) concentration ranging from 0 to 0.5 wt % and 2 wt % of MAH using twin-screw reactive extruder. Under these conditions, between 0.066 and 0.672 wt % MAH was grafted onto the PLA chains.

Radical grafting of PLA with reactive monomers affects properties of modified PLA. Enhanced reactivity of PLA-g-MAH was discussed by Pan et al. [25] as a result of highly reactive carboxylic group. Carlson et al. [26] investigated the influence of concentration of initiator on the amount of grafted MAH and molecular weight of PLA-g-MAH. Increasing concentration of initiator resulted in increasing grafting degree while molecular weight decreased due to chain scission. Thus modified PLA improved miscibility in PLA/starch blend. Hwang et al. [27] investigated the influence of concentration of initiator on physical (T_g, T_m, X_c) and mechanical (tensile strenght, Young modulus, tensile elongation) properties. Grafting with MAH resulted in decrease of glass transition temperature and crystallinity due to branching. On the other hand, mechanical properties were unchanged.

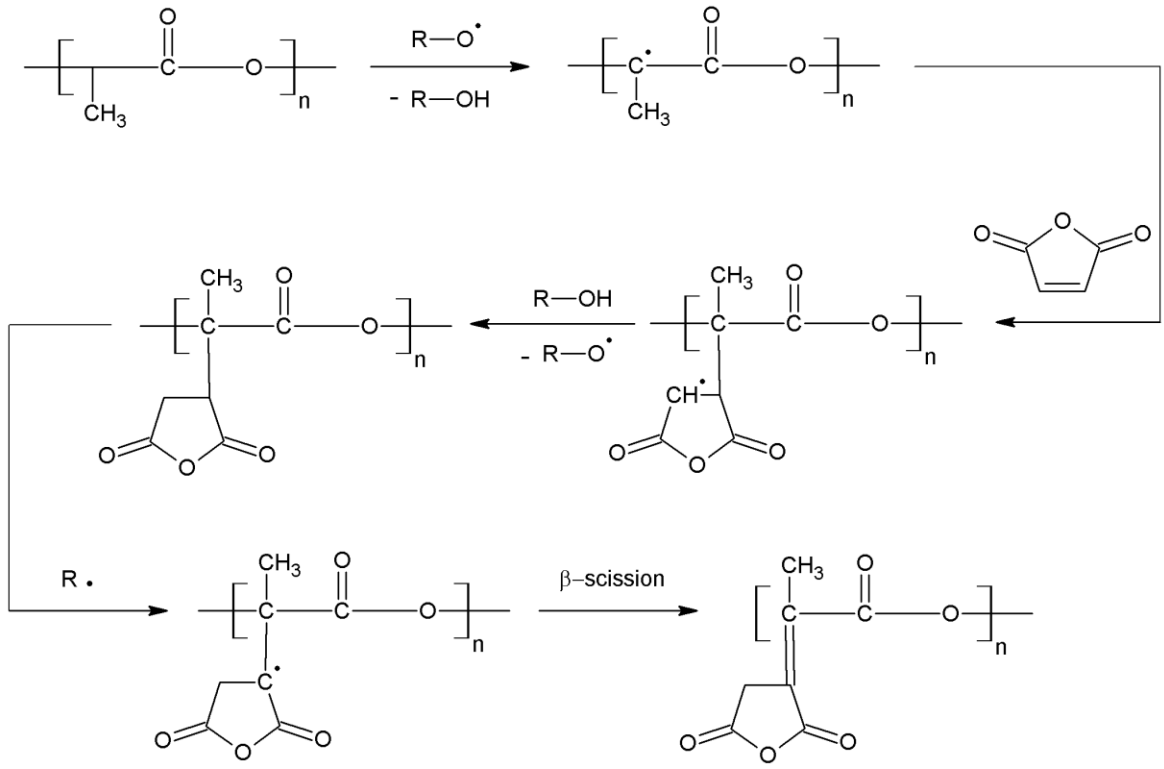

Figure 6. Scheme of maleation of PLA adapted from study Pan et al.[25].

Modified PLA can be used in composites reinforced by filler which exhibit improved biodegradability, adhesion towards filler particals and inhibited flammability.The effect of

PLA-g-MAH in biocomposites was studied by Plackett [28]. Thus prepared biocomposites exhibited enhanced adhesion towards filler in wood fibers and nanoclay. Zhang and Sun [29] focused on testing mechanic properties of PLA/starch blends which were prepared by "in situ" compounding of PLA, starch and MAH in the presence of organic peroxide initiator. To compare, composites were also prepared by compounding of PLA, starch and PLA-g-MAH. In both cases, enhanced interfacial adhesion between PLA and starch resulted in increased tensile strenght and elongation

An effort to substitute petroleum-based polymers, leads to preparation of polymer blends with high content of polymers derived from renewable resources with improved biodegradability of prepared materials [30]. On the other hand, study proposed by Reddy, Nama and Yang [31] describes preparation of PP/PLA blend in order to avoid degradation and hydrolytic scission of PLA. Authors expect possible applicability of PP/PLA fibers with respect to lower price compare to PLA fibers. Possitive effect of compatibilizer on mechanical and thermal properties of polymer blends with PLA is mentioned in several works [31]–[32].

3. AIMS OF THE WORK

The main goal of proposed thesis is preparation and characterization of PLA grafted with IAH (signed as PLA-g-IAH). Reaction compounds (PLA and IAH) derived from renewable resources in combination with reaction method without using solvent make PLA-g-IAH to be a promising material with large scale of applications.

First part of experimental section is focused on investigation of grafting reaction "in situ" using thermal analysis. The aim of this section is to describe the influence of reaction parameters on reaction course. Formation of byproducts and their decomposition will be detected during grafting reaction which is not able to observe within conventional procedure in internal mixer.

In the second part, PLA is functionalized via radical grafting with IAH in internal mixer at different concentration of reactants. Aims of this part are as follows:

1) Successful grafting of IAH onto PLA backbone, structure analysis and qualitative analysis of grafted IAH.
2) Proposition of reaction conditions and their optimization with respect to processing parameters of PLA and $\tau_{1/2}$ of chosen initiator.
3) Investigation of the influence of reaction conditions on grafting yield and extent of side reactions, possibility of IAH polymerization and structure of PLA-g-IAH.
4) Determination of kinetic parameters for selected reaction system.
5) Study of non-radical degradation of PLA during processing and its inhibition by addition of chain extender.

4. EXPERIMENTAL PART

This chapter provides detail description of materials, methods and characterization used in this thesis.

4.1 Reactants

- POLYMER: Poly(lactic acid) (PLA) Ingeo 2003D grade - NatureWorks Ltd; m. p. 150 °C; 1.24 $g \cdot cm^{-3}$; MFR (210/2.16) = 6 g/10 min.

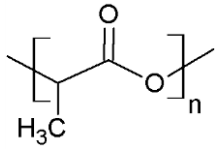

- MONOMER: Itaconic anhydride (IAH) - Fluka; M_w = 112.09 $g \cdot mol^{-1}$; m. p. 66–70 °C.

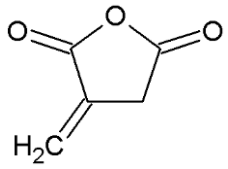

- INITIATOR: 2,5-bis(tert-butylperoxy)-2,5-dimethylhexane (L101) - Sigma-Aldrich; M_w = 290.44 $g \cdot mol^{-1}$; b. p. 55–57 °C; $\tau_{1/2}$ = 10 h (108 °C).

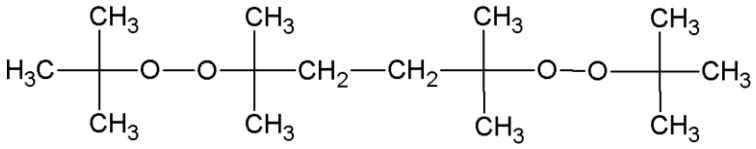

- CHAIN EXTENDER: Joncryl ADR-4368 C – BASF; M_w = 6800 $g \cdot mol^{-1}$; T_g = 54 °C; epoxy equivalent weight 285 $g \cdot mol^{-1}$.

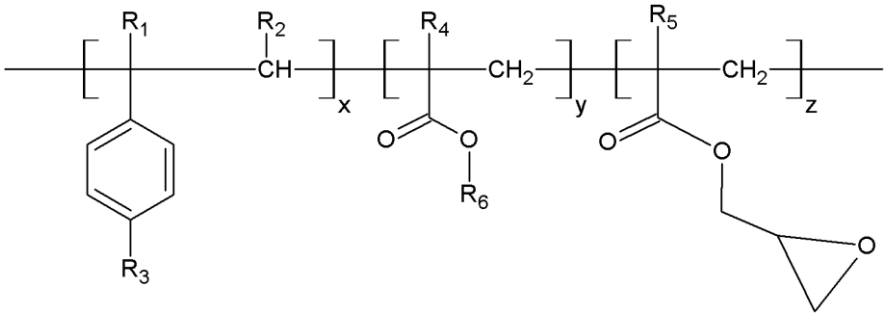

$R_{1\text{-}5}$: H, CH_3, $C_{2\text{-}10}$ alkyl group, R_6: alkyl group

4.2 Experiments overview

Melt radical grafting of PLA in internal mixer

The PLA-g-IAH was prepared via grafting reaction between PLA and IAH initiated by L101 in discontinuous internal mixer Brabender (Brabender, Germany) with 50 mL volume of reaction chamber. Reaction parameters used for reaction are summarized in Table 4. Unreacted monomer was removed by dissolving in 1,2-dichlorbenzene thus obtained polymer solution was precipitated into ethanol, filtered and dried in vacuum oven at 60 °C for 12 h.

Table 4. Overview of reaction conditions applied for radical grafting of PLA.

	$[L101]_0$ [wt %]			
$[IAH]_0$ [wt %]	**0.1**	**0.5**	**1**	**2**
0.5	0.5-0.1	0.5-0.5	0.5-1	0.5-2
1	1-0.1	1-0.5	1-1	1-2
5	5-0.1	5-0.5	5-1	5-2
10	10-0.1	10-0.5	10-1	10-2

Reaction temperature 190 °C (m. p. of PLA equals to 150 °C) was calculated for reaction time 6 min according to Arrhenius whereas after 6 min of reaction period L101 was completely decomposed as shown in exponential plot in Figure 7.

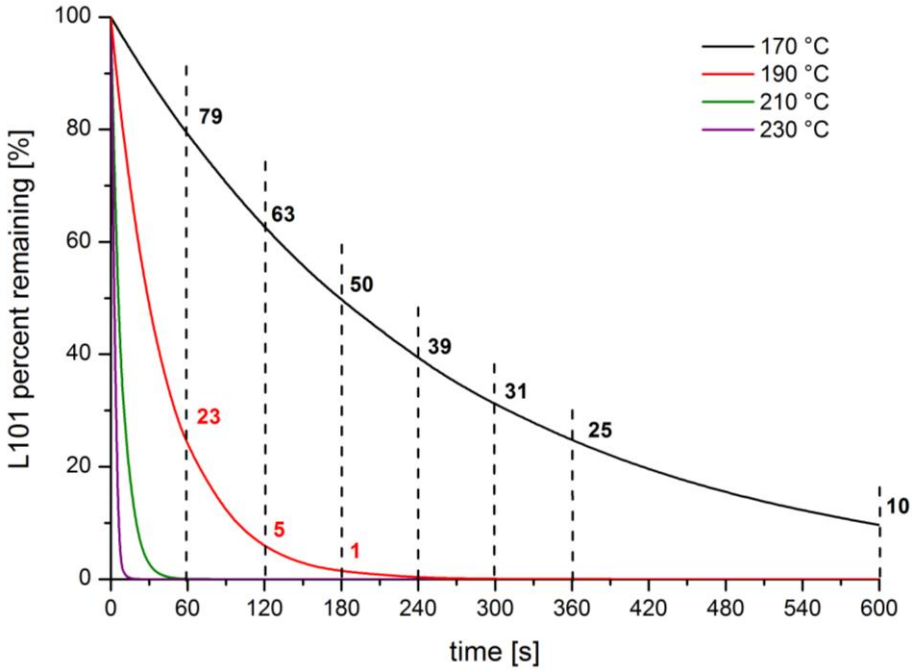

Figure 7. Calculated L101 percent remaining as a function of time determined for different reaction temperatures.

Radical reaction of PLA with IAH in the presence of chain extender

Commonly used Joncryl ADR-4368 C was chosen in order to study the influence of additive with reactive groups on rheological properties of PLA-g-IAH. Samples prepared according to reaction parametrers in Table 5 were prepared via radical reaction according procedure which is described in previous chapter. Concentration 0.5 wt % of chain extender was loaded into the polymer melt before loading of initiator.

Table 5. Summary of reaction parameters used for radical grafting of PLA in the presence of 0.5 wt % of chain extender.

	Sample			
	$[L101]_0$ [wt %]			
$[IAH]_0$ [wt %]	**0.1**	**0.5**	**1**	**2**
0.5	0.5-0.1-0.5	0.5-0.5-0.5	0.5-1-0.5	0.5-2-0.5
5	5-0.1-0.5	5-0.5-0.5	5-1-0.5	5-2-0.5

Kinetics of grafting

Kinetics of PLA grafting was study according to reaction conditions summarized in Table 6. Reaction products were purified according previous procedure by dissolving in methylenechloride and precipitation in methanol. Purified PLA-g-IAH was dried in vacuum oven for 12 h at 60 °C. Thus prepared samples were characterized via acid-base titration in order to determine amount of grafted monomer and reaction conversion. Analysis was achieved according to procedure described in chapter 4.3.

Table 6. Reaction parameters applied for study of kinetics of radical grafting of PLA.

Experiment series	**$[IAH]_0$ [wt %]**	**$[L101]_0$ [wt %]**	**T_r [°C]**	**t_r [min]**
A-170	0.5	0.1	170	1, 3, 6, 10
		0.5	170	1, 3, 6, 10
		1	170	1, 3, 6, 10
A-190	0.5	0.1	190	1, 3, 6, 10
		0.5	190	1, 3, 6, 10
		1	190	1, 3, 6, 10
A-210	0.5	0.1	210	1, 3, 6, 10
		0.5	210	1, 3, 6, 10
		1	210	1, 3, 6, 10

Extraction of low molecular weight fractions

Low molecular weight fractions were extracted from raw PLA-g-IAH samples by extraction in aceton at room temperature for 48 h. Solvent was evaporated under atmospheric pressure and

thus prepared powdered samples were overdried in vacuum oven at room temperature. Thus obtained extracts were used for further characterization.

Investigation of radical grafting "in situ"

Radical grafting was also study "in situ" by differential scanning calorimetry (DSC) and thermogravimetric analysis (TGA). Concentrations of monomer and initiator were used according to Table 4, chapter 4.2. PLA/IAH/L101 mixtures with different $[IAH]_0$ and $[L101]_0$ were prepared by impregnation of IAH and L101 onto PLA powder and thus prepared samples were used for analysis.

Grafting reaction was studied via DSC run (TA Instruments 2920) achieved in temperature range from 30 to 210 °C at heating rate of 5 °C/min under nitrogen atmosphere. Raw data were processed by TA Universal Analysis software.

TGA was used for qualitative analysis of decomposition products released during grafting reaction. Desired amount of powdered sample was loaded into the platinum pan and reaction was achieved in the temperature range from room temperature to 240 °C and a heating rate 5 °C/min and consequently from 240 °C to 500 °C and a heating rate 10 °C/min.

Simulation of side reactions

Homopolymerization of IAH

Possible IAH homopolymerization was simulated via reactions between IAH and L101 and was achieved in glass tubes at conditions similar to those applied in grafting reactions described in chapter 4.2. Glass tube was heated in oil bath at 190 °C. After oil bath reached desired temperature, IAH/L101 mixture was place into the glass tube in given IAH/L101 ratio which is shown in Table 7 as well as other reaction parameters.

Solution polymerization of IAH in the presence of AIBN as an initiator was achieved in order to prepare (p(IAH)) according to well known procedure giving sufficient polymerization yield [39], [50]. Polymerization of IAH was accomplished by modified method published by Otsu and Yang [46]. IAH was polymerized in ethyl acetate at 80 °C for 12 h in the presence of AIBN radical initiator (4 mole % with respect to monomer). Thus prepared p(IAH) was precipitated in toluene and dried at 80 °C for 10 h.

Table 7. Reaction parameters applied for side reaction between IAH and L101.

Signification	nIAH/nL101 [mol/mol]	T_r [°C]	t_r [min]
2.59	2.59	190	6
5.18	5.18		
25.91	25.91		
51.28	51.28		
129.56	129.56		
259.11	259.11		

Reactions between PLA and primary radicals

Reaction between PLA and L101 was studied via reaction without IAH in internal mixer at 187.4 °C and 6 min residence time. Concentrations of L101 were in agreement with those given in Table 4, chapter 4.2 (0.1–2 wt %).

IAH isomerization

Possible IAH isomerization onto citraconic anhydride (CAH) was study via reaction achieved in glass tube at 80, 100, 120, 140, 160 and 180 °C for 6 min residence time. And thus prepared samples are signed as "IAH 80", "IAH 100", etc. etc.

4.3 Characterization methods

Structure analysis

Characteristic functional groups of PLA-g-IAH were observed by Fourier transform infrared spectroscopy (FTIR) and compared to FTIR spectrum of neat PLA. Samples were analyzed using FTIR spectrometer (Bruker) in ATR measuring mode (32 scans, resolution 4 cm^{-1}).

Nuclear magnetic resonance (^{1}H-NMR) was used to estimate structure of PLA-g-IAH and confirm the presence of grafted monomer. Polymer solution was put into the test tubes and measured using Varian 500 MHz spectrometer.

Grafting yield determination

Grafting yield was determined by acid-base titration carried out with 0.005N potassium hydroxide (KOH) in ethanol and 1% thymol blue in ethanol as an indicator. Grafting degree $[IAH]_{PLA}$ was calculated according to Equation 4:

$$[IAH]_{PLA} = \frac{c_{KOH} \cdot (V_{KOH} - V_{blank}) \cdot M_{IAH} \cdot \frac{1}{2}}{m_v} \cdot 100 \quad [wt\ \%] \tag{4}$$

where c_{KOH} is concentration of KOH solution (mol·L^{-1}); V_{KOH} and V_{blank} (mL) is the volume of KOH solution at equivalence point for the PLA-g-IAH and neat PLA, respectively; M_{IAH} is molecular weight of IAH (g·mol^{-1}); m_v is the weight of the sample used for analysis (g). Since different –COOH groups can be presented in PLA-g-IAH solution, neat PLA was titrated in order to minimize innacurancy of quantification of grafted IAH

Rheological properties

The melt flow index of PLA-g-IAH and neat PLA was measured by Melt Flow Tester Ceast (Ceast MMF 70-24.000, Italy). Approximately 6 g of sample were loaded into the heated barrel equipped with capillary and the measuring was performed at 190 °C and load 2.16 kg according to ISO 1133D standard method.

Flow curves for chosen PLA-g-IAH samples prepared with and without addition of chain extender were measured by the same device as for regular melt flow index measurement. Four different loadings were applied depending on viscosity of polymer melt: 1.2, 2.16 and 3.8 kg for samples without chain extender, 2.16, 3.8 and 5 kg for samples prepared in the presence of chain extender.

Viscometric measurements of PLA-g-IAH solutions were carried out using Ubbelohdeho viscometer. The concentration of PLA-g-IAH solutions covered 1–20 g/L. All measurements were carried out at 30 ± 0.1 °C where all measured solutions were tempered at least for 30 minutes before measuring. Each sample was measured three times for good reproducibility. Thus obtained concentration-viscosity was extrapolated to zero concentration to obtain intrinsic viscosity to deduce molecular weight of tested PLA-g-IAH samples.

Molecular weight determination

Size exclusion chromatography SEC was used to determine changes of molecular weight due to grafting reaction. Approximately 1 mg of purified PLA-g-IAH samples was dissolved in 1 ml of THF and ca 0.8 mL of each sample solution was injected into the SEC chromatograph (Waters, USA) through the 0.45 μm filter to remove non-dissolved fragments which may block the system. Flow rate 0.5 $mL \cdot min^{-1}$, run time 30 min and temperature 35 °C were applied.

Thermal properties

Thermal properties of prepared samples such as glass transition temperature T_g, melting temperature T_m, cold crystallization temperature T_{cc} and percent crystallinity X_c were determined using differential scanning calorimeter DSC (Netzsch, Germany). Analysis was achieved in temperature range from 20 to 220 °C at heating rate of 20 °C/min and 10 °C/min during first and second heating cycle, respectively. All measurements were carried under nitrogen atmosphere. Mentioned phase transitions were determined using Netzch software (Netzsch Proteus thermal analysis) and the X_c was calculated using the following Equation 5:

$$X_c = \frac{\Delta H_m - \Delta H_c}{\Delta H_m^o} \cdot 100 \quad [\%] \tag{5}$$

where ΔH_m, ΔH_c and ΔH_m^o ($J \cdot g^{-1}$) are enthalpies of fusion, enthalpy of cold crystallization and enthalpy of fusion of 100% crystalline PLA (93.1 $J \cdot g^{-1}$), respectively [57].

Thermal stability

Thermal stability was carried out using TA instruments Q500 device. Thermogravimetric analysis (TGA) was carried out under nitrogen atmosphere from room temperature to 500 °C and a heating rate of 10 °C/min. Raw and purified PLA-g-IAH samples were used for analysis.

Biodegradation test

Purified PLA-g-IAH foils used for degradation test were prepared by evaporation of solvent (THF). Thus prepared samples were placed into glass vials and 4 ml H_2O was added. The pH values of suspension liquor were measured once a week for 12 weeks using pH meter S2K712 (ISFETCOM, Japan).

Colorimetric analysis

Color change of unpurified PLA-g-IAH was measured by X-rite i1 spectrophotometer in visible spectrum 380–760 nm. Approximately 450 ± 20 μm thick foils were used for measurement while each sample was measured five times for susceptible reproducibility.

Contact angle measurement

Contact angle tester (rame-hart Model 250) was used to predict the influence of grafted IAH on hydrophilic properties and surface tension of PLA-g-IAH. Polymer films of non-purified samples were prepared by evaporation of THF from polymer solution and thus prepared PLA-g-IAH films were used for analysis.

5. RESULTS AND DISCUSSION

5.1 Prediction of grafting mechanism

As mentioned in the theoretical background, radical grafting is a complex of reactions which occur simultaneously with the main grafting reaction. Generally, these reactions can be split on desired main grafting reaction and undesired side reactions which complicate grafting process. The main grafting reaction is schemed vertically in the Scheme 1 and contains following reaction steps: a) thermal decomposition of initiator (L101) according to reaction 1 and generation of primary radicals which may be decomposed on secondary radicals (reaction a1) - both types of radicals signed as L101$^{\bullet}$; b) PLA macroradicals formation (PLA$^{\bullet}$) by hydrogen abstraction mainly from tertiary carbon of PLA backbone (reaction 2); c) covalent bonding of monomer (IAH) onto PLA$^{\bullet}$ (reaction 3); d) termination of grafting by hydrogen donors (reaction 4). Proposed reaction sequence leads to preparation of PLA modified with IAH, in this thesis signed as PLA-g-IAH.

Main grafting reaction is limited by several side reactions which may occur during functionalization depending on reaction conditions (e.g. initiator and monomer concentration, reaction temperature, reactivity of generated radicals, etc.). Most important side reactions are expected and horizontally schemed in the Scheme 1.

Except of hydrogen atom abstraction, L101$^{\bullet}$ (formed in reaction 1 and 1a) can either recombine (reaction 1b) or interact with IAH forming inactive species and IAH radicals (IAH$^{\bullet}$), respectively. Both reactions decrease grafting yield. Moreover, it is expected that secondary methyl radicals are more favoured to participate on IAH homopolymerization via addition to IAH double bond (reaction 1a) compared to bulky t-butoxy radicals.

PLA$^{\bullet}$ generated according to reaction 2 can undergo several reactions which may affect flow properties and mechanical properties. Due to reaction between PLA$^{\bullet}$ and L101$^{\bullet}$, active centers become inactive for grafting (reaction 2a). Coupling reactions between PLA$^{\bullet}$ cause crosslinking (reaction 2b) which influences solubility and gel content. Degradation reaction 2c represents β-scission with subsequent radical branching (reaction 2ca).

When IAH is bonded on PLA backbone, reactive center located in the structure of bonded IAH can be deactivated in several ways. PLA-g-IAH radicals (PLA-g-IAH$^{\bullet}$) are perished by interactions with other radical species (reaction 3a), coupling with another PLA-g-IAH$^{\bullet}$ (reaction 3b) or homopolymerization on PLA chain (reaction 3c).

Molecular weight of PLA-g-IAH can decrease although grafting degree increases. This may occur due to presence of labile hydrogen atom on tertiary carbon of grafted IAH which can be abstracted by radical species. Thus formed PLA-g-IAH may undergo β-scission according to Scheme 1.

Except of radical reactions, non-radical reactions participate on the grafting process and affect properties of functionalized PLA. These reactions are based on the nature of PLA and will be discussed below.

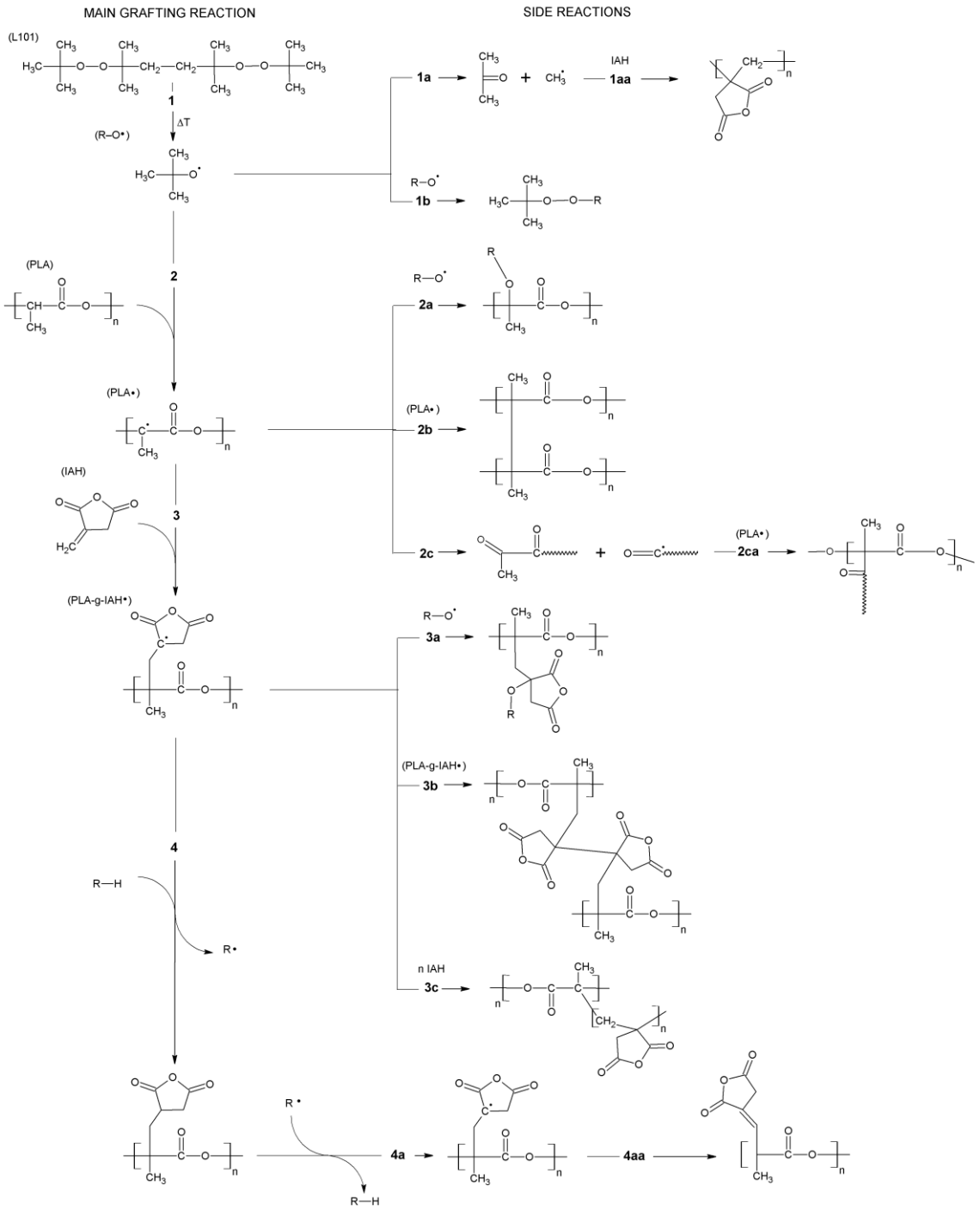

Scheme 1. Expected main grafting reaction including: generation of primary radicals via thermal decomposition of L101 (1); hydrogen abstraction from PLA backbone (2); addition of IAH onto PLA (3); termination of grafting (4). Possible side reactions: formation of secondary methyl radicals (1a) and possible IAH homopolymerization (1aa); primary radicals recombination (1b); extinction of active center on PLA backbone (2a); crosslinking (2b); β-scission (2c) with subsequent radical branching (2ca); addition of radicals on PLA-g-IAH• (3a); coupling of PLA-g-IAH• (3b); homopolymerization of grafted IAH (3c); hydrogen abstraction from PLA-g-IAH (4a) with subsequent β-scission (4aa).

5.2 Investigation of PLA grafting "in situ"

Radical grafting of PLA with IAH was investigated "in situ" using DSC in the temperature range 30–220 °C at heating rate 5 °C/min. Different $[IAH]_0$ and $[L101]_0$ were applied according to concentrations of reactants used for grafting reaction achieved in internal mixer (Table 4, chapter 4.2). DSC thermogram typical for "in situ" grafting reaction is shown in Figure 8a. DSC curve of each sample consists of three phenomena: a) glass transition of PLA at ~50 °C; b) melting of PLA reflected by endothermic peak at ~150 °C; c) broad exothermic peak attributed to grafting reaction in melt. Dashed curve in Figure 8 represents decreasing content of L101 which was calculated regarding heating rate. L101 is completely consumed at ~180 °C which corresponds with maximum of exothermic peak reflecting grafting reaction. Below this temperature, reaction conversion increases as both reaction time and concentration of $L101^{\bullet}$ increase. Above 180 °C, decrease of reaction rate is expected due to absence of $L101^{\bullet}$ while termination reactions are prefered.

Although many authors do not expect simultaneous IAH homopolymerization due to high processing temperature, configuration of DSC experiments allows predicting IAH homopolymerization occuring simultaneously with main grafting reaction. DSC curves in Figure 8a–d represent reaction system with 0.5–10 wt % of IAH and 0.1–2 wt % of L101. As mentioned above, each DSC curve exhibits exothermic peak in the range 160–210 °C which reflects overall grafting reaction. Reaction system with 0.1 and 0.5 wt % of L101 contains exothermic peak which is signifficantly separated from the endothermic peak reflecting PLA melting. On the other hand, DSC curves of reaction system containing 1 and 2 wt % L101 does not exhibit sharp boundary between endothermic melting and exothermic grafting. This phenomenon may suggest hypothesis that homopolymerization of IAH occurs at lower temperature compared to main grafting reaction.

Hypothesis described above is based on the fact that melting of PLA occurs in the temperature range 110–160 °C depending on the molecular weight of melted polymer and polydisperzity of system. Concentration of primary radicals is expected to be low in this temperature range with respect to high $\tau_{1/2}$ of L101 in this temperature range. Consequently, IAH homopolymerization can be expected and p(IAH) could be formed. At relatively lower temperature (around PLA melting), low mobility of polymer chains retards grafting reaction. Low bulky IAH molecules with high mobility can thus interact with $L101^{\bullet}$ whereas their relatively high mobility allows formation of p(IAH). Although high mobility of low molecules could support their interactions, high concentration of polymer chains and tertiary carbons prefers reaction between PLA and $L101^{\bullet}$. Consequently, high $[IAH]_0$ and $[L101]_0$ could enhance the extent of interactions between IAH and $L101^{\bullet}$ which would raise yield of IAH homopolymerization.

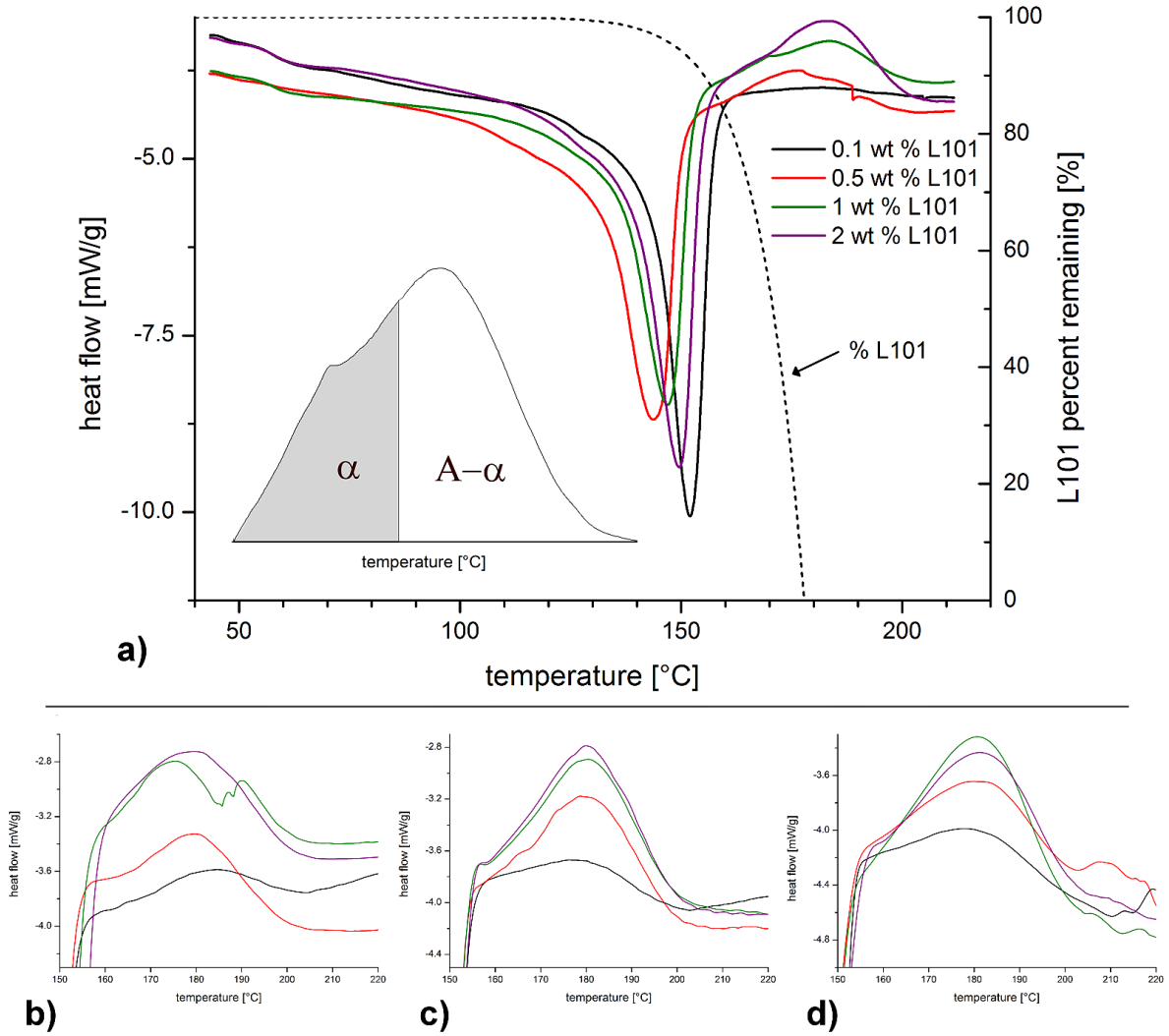

Figure 8. "In situ" investigation of PLA grafting with IAH: DSC thermogram representing thermal response of grafting reaction of samples 0.5-x (a), 1-x (b), 5-x (c) and 10-x (d) where x = $[L101]_0$ = 0.1–2 wt %; part (a) includes schematic illustration of observed exothermic peak attributed to heat of reaction vs. temperature for grafting reaction.

Depending on the $[IAH]_0$ and $[L101]_0$, heat of reaction ΔH_r changes. 3D plot in Figure 9 illustrates the influence of concentration of reaction compounds on heat evolving during reaction. It can be assumed that heat of reaction relates to reaction composition and increases with increasing $[IAH]_0$ and $[L101]_0$. As $[IAH]_0$ is constant, heat of reaction increases rapidly with increase of $[L101]_0$. Observed relationship is in good agreement with previous assumption that higher $[L101]_0$ supports formation of $PLA^{\bullet}$ with subsequent bonding IAH. When $[L101]_0$ is low (i.e. 0.1 wt %), ΔH_r slightly increases (1.7–4.9 $J.g^{-1}$) with increasing $[IAH]_0$. At these reaction conditions, grafting degree reached 0.18–0.88 wt % (see Figure 12, chapter 5.4.1). It can be concluded that total heat of reaction can be evolved mainly from grafting reaction. On the other hand, two main differences should be mentioned. First, efficiency of radical grafting achieved in internal mixer was supported by intensive homogenization during processing. Instead of this,

calorimetric study of PLA grafting is strongly dependent on diffusion of reaction compounds as well as on their mobility. From this reason, reactions of bulky radicals are more disadvantaged. Second, total heat of reaction represents sum of heats of individual side reactions which were mentioned in previous text. Especially at high $[IAH]_0$, homopolymerization may affect total heat of reaction althogh it is not usually expected due to high operating temperature.

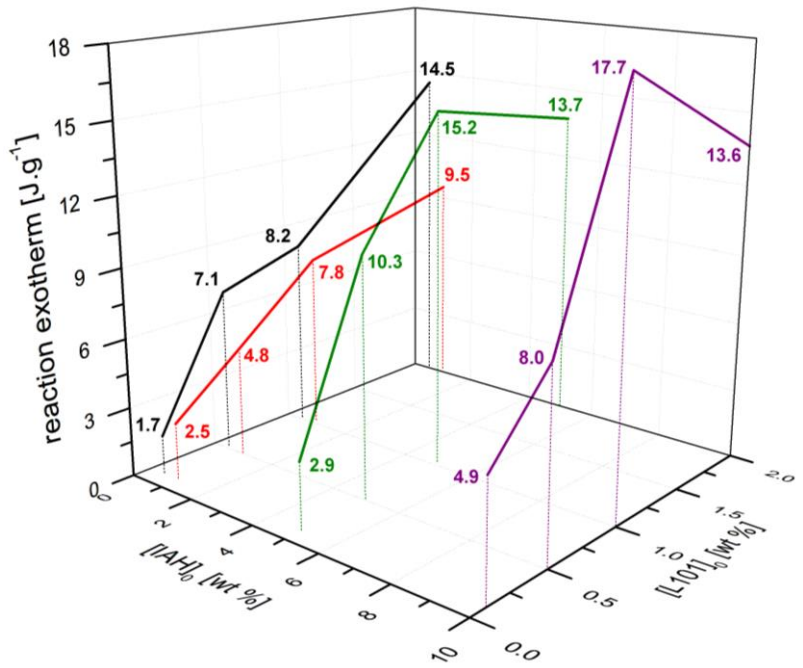

Figure 9. Relationship $[IAH]_0$-$[L101]_0$-ΔH_r derived from DSC thermogram obtained during „in situ" calorimetry grafting.

The heat of grafting reaction determined for reaction system with constant $[L101]_0$ does not increase so rapidly with increasing $[IAH]_0$. It can be concluded that at low $[IAH]_0$, secondary reactions occur, i.e. crosslinking and chain branching. Based on the heat evolved during reaction, these undesired reactions exhibit higher reaction enthalpy compared to reactions that predominate at high $[IAH]_0$.

5.3 Evidence of IAH grafted onto PLA backbone

Structure of modified PLA was examined by Fourier transform infrared spectroscopy (FTIR). Expected structure of prepared grafted PLA is illustrated on reaction mechanism in Scheme 1 as a product of Scheme 1 included in the sequence of main grafting reaction.

FTIR spectrum of neat PLA and PLA-g-IAH is shown in Figure 10a. Detail of PLA-g-IAH's FTIR spectrum contains absorption bands at around 2860 and 2920 cm^{-1} which can be assigned to $–CH_2$ functional groups, respectively (Figure 10b). Appearance of $–CH_2$ groups can be considered as proof of grafted IAH (Scheme 1, reaction 3) whereas $–CH_2$ groups are included in molecule of IAH.

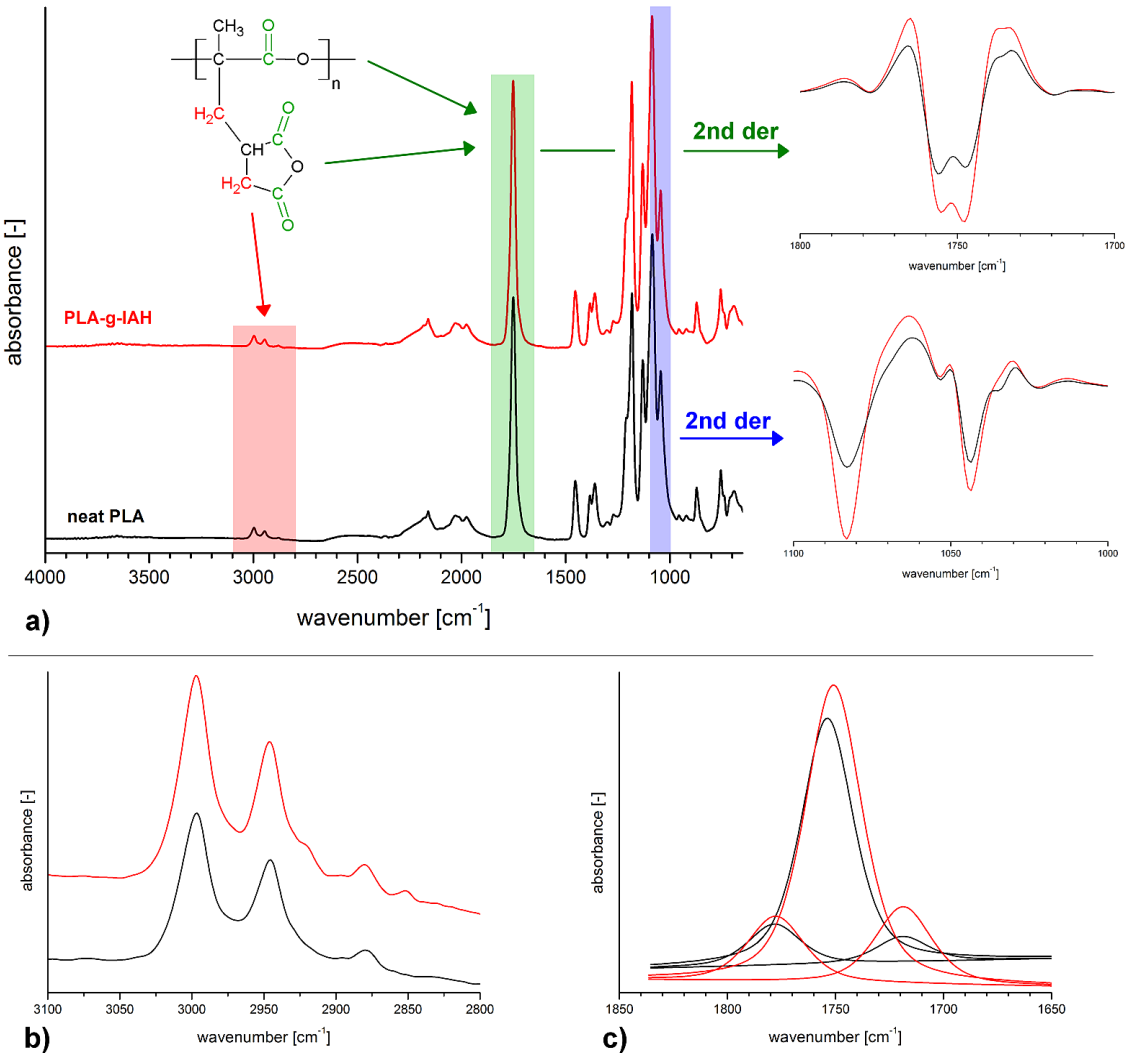

Figure 10. FTIR spectrum of neat PLA and PLA-g-IAH in the wavenumber range 4000–650cm^{-1} with 2nd derivative spectra in the wavenumber range 1800–1700 and 1100–1000 cm^{-1} (a); detail of absorption bands in the wavenumber range 3100–2800 cm^{-1} (b) and 1850–1650 cm^{-1} (c).

FTIR spectrum of PLA-g-IAH does not exhibit any different absorption band in the region typical for C=O vibrations (1600–1800 cm^{-1}) compared to neat PLA. Strong absorption band centered at 1750 cm^{-1} is composed of several types of C=O vibrations which may represent both PLA and grafted IAH. It can be predicted that C=O absorption bands of IAH are overlapped due to low concentration of grafted IAH. Therefore, 2nd derivave FTIR spectra were obtained in order to enhance resolution of overlapped peaks which were not observed in native spectra. This method was applied in study Mani, Bhattacharya and Tang [20] dealing with preparation and characterization of polyesters modified with MAH. Accordingly, authors splitted FTIR signal using 2nd derivation which improved resolution of FTIR spectra. New absorption bands at 1785 cm^{-1} were observed due to presence of bonded MAH on polyester backbone.

The example of 2nd derivative FTIR spectrum is depicted in Figure 10a and contains characteristic peaks in wavenumber range of 1700–1800 cm^{-1} for both PLA and PLA-g-IAH:

peak at 1780 cm^{-1} belongs to C=O stretching vibration of ester bond; strong peak at 1760 cm^{-1} is characteristic for C=O stretching vibration; peak at 1740 cm^{-1} assigned to C=O stretching vibrations of carboxylic group; peak at 1730 cm^{-1} characteristic for C=O stretching vibration of ester bond. The difference between 2nd derivative spectra of PLA and PLA-g-IAH was observed in the wavenumbers range 1000–1100 cm^{-1}. FTIR spectrum of neat PLA exhibits peak at 1035 cm^{-1} which is characteristic for C–O stretching of C–OH bond appeared as a result of PLA thermohydrolysis [26]. As will be discussed in next section, chain scission of neat PLA can occur via non-radical degradation such as hydrolysis and thermal degradation whereas β-scission can be promoted by reaction between PLA and $L101^{\bullet}$. Consequently, it can be assumed that β-scission predominates over the non-radical degradation during reactive modification of PLA.

As discussed above, absorption band centered at around 1760 cm^{-1} includes C=O vibrations of cyclic anhydride group. Due to low concentration of grafted IAH, single peak reflecting C=O stretching vibration of anhydride ring was not observed. Therefore, FTIR spectra of neat PLA and PLA-g-IAH were normalized to the peak at 1167 cm^{-1} which represents C–C stretching vibration between $–CH_3$ group and tertiary carbon of PLA backbone. Constant content of CH_3 groups was expected due to lower reactivity of primary $–CH_3$ compared to tertiary –CH defined by strength of C–H bond. Increasing integral intensity of absorption band relating to C=O stretching vibration at 1780 cm^{-1} was observed for PLA-g-IAH compared to neat PLA. Figure 11 contains $A_{PLA\text{-}g\text{-}IAH}/A_{neat\ PLA}$ values obtained for PLA-g-IAH samples prepared at constant $[IAH]_0$ (1 and 5 wt %) and different $[L101]_0$ (0.1–2 wt %). An increase of $A_{PLA\text{-}g\text{-}IAH}/A_{neat\ PLA}$ for C=O absorption band at 1760 cm^{-1} is assigned to effect of IAH bonded on the PLA backbone. This can be considered as a proof of bonded IAH in purified PLA-g-IAH.

In order to prove method of peak normalization, PLA/IAH blends were prepared by blending with defined amount of IAH (0.5, 1, 5 and 10 wt %) in THF. Obtained FTIR spectra were normalized to absorption band at 1167 cm^{-1} according to method used for PLA-g-IAH samples. FTIR spectra of PLA/IAH blends are shown in Figure 11 as well as derived values of $A_{PLA\text{-}g\text{-}IAH}/A_{neat\ PLA}$ for C=O absorption band at 1760 cm^{-1}. It was observed that $A_{PLA\text{-}g\text{-}IAH}/A_{neat\ PLA}$ increases with increasing concentration of IAH in PLA/IAH blend. Moreover, FTIR spectra of PLA/IAH blends with 5 and 10 wt % IAH contain weak absorption band at 1850 cm^{-1} relating to C=O stretching vibrations of IAH. Described absorption band was not observed for PLA/IAH blends with IAH concentration below 5 wt %. As discussed in chapter 5.4.1, maximum grafting degree 1.1 wt % was reached. It means that FTIR spectra contain C=O stretching vibrations of IAH at 1780 cm^{-1} overlapped in the wavenumber range 1700–1800 cm^{-1} while C=O stretching vibrations at 1850 cm^{-1} cannot be observed due to low concentration of grafted IAH.

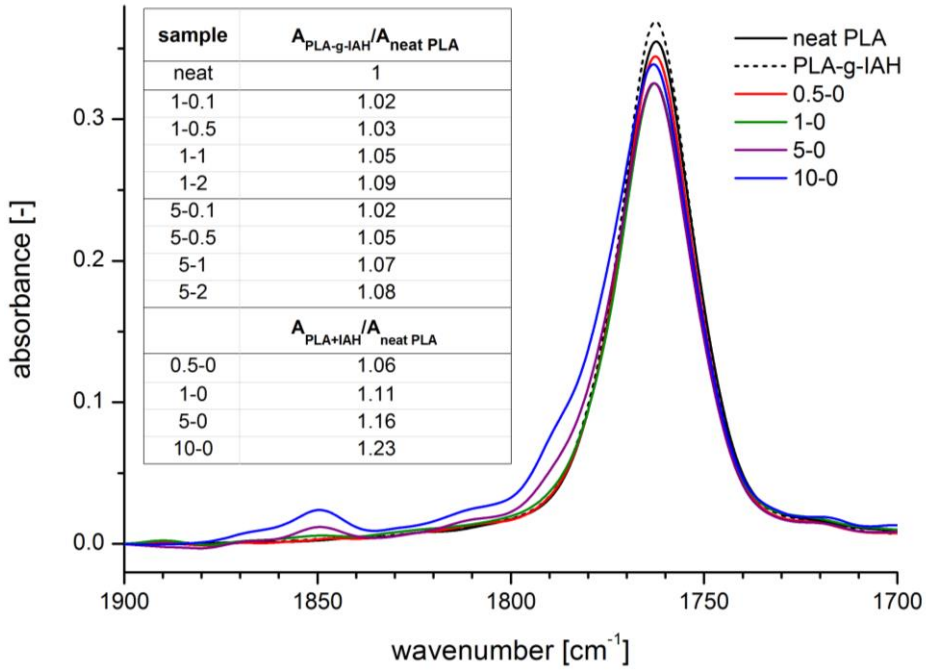

Figure 11. Detail of FTIR spectrum of neat PLA, PLA-g-IAH and PLA/IAH blends with different $[IAH]_0$ – peak at 1760 cm^{-1} (stretching vibrations of C=O) normalized to peak at 1167 cm^{-1} (stretching vibrations of CH_3).

5.4 Reaction parameters affecting grafting yield

Mechanism of radical grafting was described in chapter 5.1. Radical grafting of IAH onto PLA may consist of several reactions occuring simultaneously. Extent of these side reactions depends on reaction conditions (especially concentration of reaction compounds and reaction temperature) and strongly influences grafting yield and course of the reaction.

5.4.1 Concentration of reactants affecting grafting yield

Figure 12 represents 3D plot giving relationship between concentration of grafted IAH ($[IAH]_{PLA}$) and concentration of reactants ($[IAH]_0$ and $[L101]_0$) which was determined for PLA-g-IAH samples prepared according to reaction conditions summarized in Table 4, chapter 4.2. Grafting yield is represented by conversion-$[IAH]_0$-$[L101]_0$ relationship in Figure 13. With regard to obtained data, it can be assumed that increase of $[IAH]_{PLA}$ can be assigned to increase of $[L101]_0$ in the whole range 0.5–10 wt % IAH. This is in good agreement with assumption that generation of PLA$^{\bullet}$ is favoured at high $[L101]_0$. Thus formed PLA$^{\bullet}$ allow covalent bonding of IAH (Scheme 1, reaction 3). Generally, $[IAH]_{PLA}$ increases with increasing $[IAH]_0$ while conversion degree decreases which suggests higher content of low molecular fractions including unreacted monomer or its homopolymer with respect to ceiling temperature for IAH polymerization. The highest $[IAH]_{PLA}$ was obtained for samples with 10 wt % IAH and

0.5 wt % $[L101]_0$ while highest conversion was reached for reaction with 1 wt % IAH and 2 wt % L101.

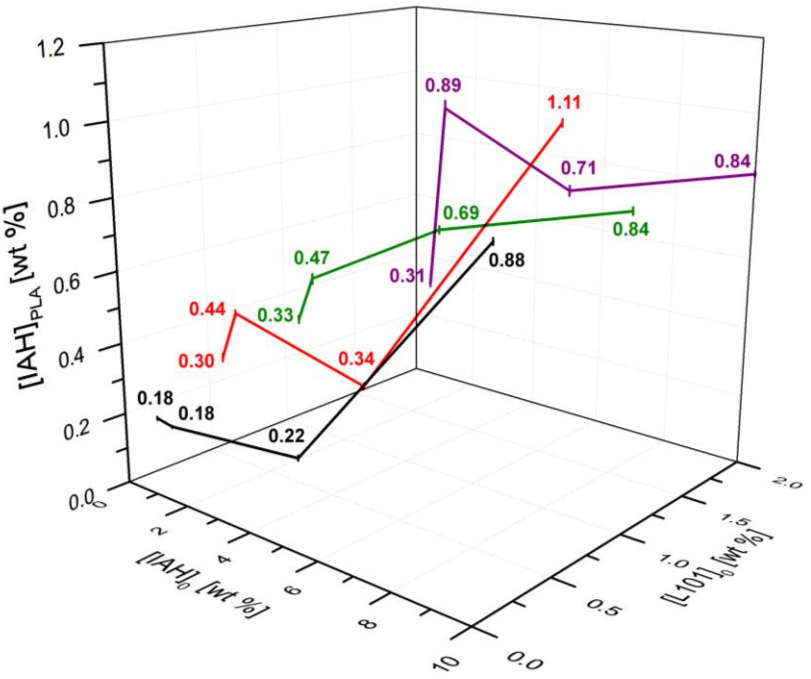

Figure 12. 3D plot representing $[IAH]_{PLA}$-$[IAH]_0$-$[L101]_0$ relationship; 0.5–10 wt % IAH; 0.1–2 wt % L101.

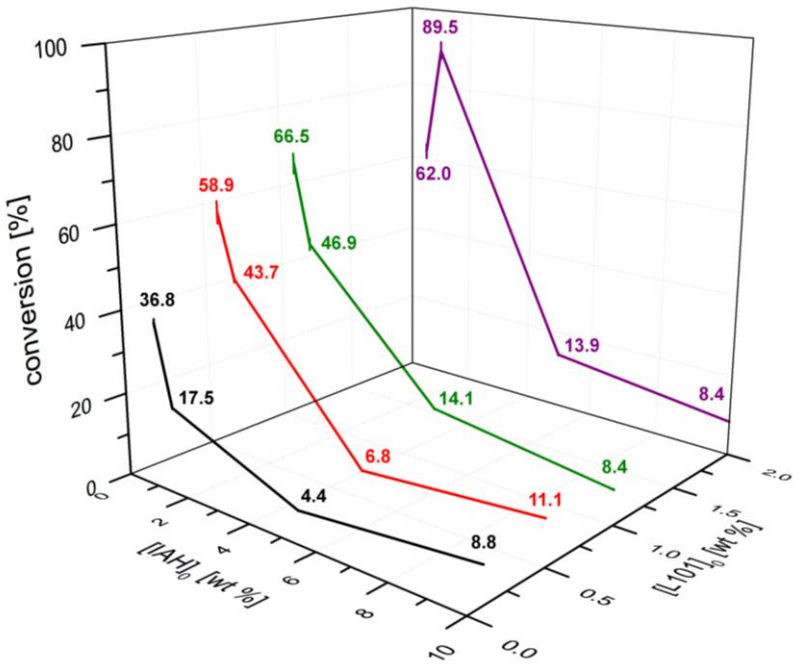

Figure 13. 3D plot representing conversion-$[IAH]_0$-$[L101]_0$ relationship; 0.5–10 wt % IAH; 0.1–2 wt % L101.

Low $[IAH]_0$ (0.5–1 wt %) and low $[L101]_0$ (0.1–0.5 wt %)

At $[IAH]_0$ equals to 0.5 wt %, $[IAH]_{PLA}$ reached plateau at 0.5 wt % of $[L101]_0$. This fact can be explained by the hypothesis that monomer was consumed mainly for grafting reaction (conversion up to ~60 %). At low $[IAH]_0$ and $[L101]_0$, probability of IAH-L101$^{\bullet}$ interactions is low even though relatively high mobility of both IAH and L101$^{\bullet}$. IAH-L101$^{\bullet}$ interactions are limited because of high concentration of tertiary carbons of PLA backbone. Consequently, formation of PLA$^{\bullet}$ is favoured and IAH homopolymerization can be neglected under these conditions. Relatively high grafting yield was determined at low $[IAH]_0$ and $[L101]_0$, therefore low extent of side reactions can be predicted.

Low $[IAH]_0$ (0.5–1 wt %) and high $[L101]_0$ (1–2 wt %)

At low $[IAH]_0$ and high $[L101]_0$, desired reaction between PLA and L101$^{\bullet}$ predominates over IAH-L101$^{\bullet}$ interactions due to several factors. First, high concentration of reactive species and –CH carbons is available for reaction with primary radicals leading to formation of PLA$^{\bullet}$ (Scheme 1, reaction 2). Second, high melt viscosity of PLA reduces extent of reactions between IAH and L101$^{\bullet}$ due to physical barrier. Third, higher amount of PLA macroradicals allows further increase of $[IAH]_{PLA}$ which was observed for PLA-g-IAH prepared by reaction with 1 wt % IAH. In this case $[IAH]_{PLA}$ increased in the whole $[L101]_0$ range. As $[L101]_0$ increases, concentration of PLA$^{\bullet}$ increases which enhances the extent of β-scission, branching or crosslinking (reactions 2c, 2ca and 2b in Scheme 1) affecting grafting degree as well as rheological and thermal properties. We just have to note that kind of interactions between radical species and their probability is strongly affected by characteristic parameters such as reactivity, solubility parameter and melt viscosity.

As $[L101]_0$ is high, L101$^{\bullet}$ can also undergo coupling while inactive species are formed according to Scheme 1, reaction 1b. Moreover, grafting yield is also limited by interactions between PLA$\bullet$ and L101$^{\bullet}$ (Scheme 1, reaction 2a). L101$^{\bullet}$ formed via thermal decomposition of L101 can participate on termination of grafting reaction via interactions with PLA-g-IAH$^{\bullet}$ (Scheme 1, reaction 3a). However, reactions between L101$^{\bullet}$ and PLA-g-IAH$^{\bullet}$ do not affect grafting yield so intensive compared to other mentioned side reactions.

High $[IAH]_0$ (1–10 wt %) and low $[L101]_0$ (0.5–1 wt %)

When $[IAH]_0$ is above 1 wt % and $[L101]_0$ is up to 0.5 wt %, $[IAH]_{PLA}$ increases significantly. Under these conditions, recombination of L101$^{\bullet}$ is not so probable and high $[IAH]_0$ supports main grafting reaction. However, reaction conversion is low due to high amount of unreacted monomer. Low grafting degree can be attributed to "cage effect" where L101$^{\bullet}$ are surrounded by IAH molecules. In that case, formation of low reactive IAH$^{\bullet}$ is preferable to grafting according to Scheme 1 (reaction 1b). Consequently, formation of p(IAH) could be possible with respect to the thermodynamic criteria.

Although low concentration PLA$^{\bullet}$ is expected due to low concentration of L101$^{\bullet}$, PLA$^{\bullet}$ can be regenerated according to reaction 4 in Scheme 1. In this scheme, RH can represent PLA which

may supply hydrogen atom for regeneration of PLA$^{\bullet}$. This reaction can be responsible for enhanced grafting degree.

High $[IAH]_0$ (1–10 wt %) and high $[L101]_0$ (1–2 wt %)

At high $[IAH]_0$ and $[L101]_0$, reaction between IAH and L101$^{\bullet}$ (Scheme 1, reaction 1aa) affects reactive process more extensively. These reactions generate low reactive IAH$^{\bullet}$ which are able to polymerize or recombine with other radical species.

Similar value of solubility parameter δ of both IAH and L101 supports IAH-L101$^{\bullet}$ interactions leading to formation of IAH$^{\bullet}$ which have potential to polymerize depending on the reaction temperature. Solubility behavior of L101 is characterized by δ equals to 15.5 $J^{1/2}\cdot cm^{-3/2}$ [40] which is close to δ of IAH (14.6 $J^{1/2}\cdot cm^{-3/2}$). Compared to this, δ of PLA (20.2 $J^{1/2}\cdot cm^{-3/2}$) [41] makes IAH-L101$^{\bullet}$ interactions more favoured compared to PLA-L101$^{\bullet}$ and PLA$^{\bullet}$-IAH interactions. This theoretical prediction corresponds with results illustrated in Figure 12 where $[IAH]_{PLA}$ decreases with increasing $[L101]_0$ when high $[IAH]_0$ is applied. Although highest $[IAH]_{PLA}$ was reached at high $[IAH]_0$, highest reaction conversion was observed for samples with low $[IAH]_0$ (Figure 13). As mentioned previously, increase of $[IAH]_{PLA}$ with increasing $[L101]_0$ can be assigned to preferable formation of PLA$^{\bullet}$ according to reaction 2 in Scheme 1. In ideal case, high $[IAH]_0$ would enhance extent of PLA$^{\bullet}$-IAH interactions leading to high reaction conversion. Though, high $[L101]_0$ does not result in significant increase of reaction conversion when $[IAH]_0$ is above 1 wt %. This situation occurs due to high $[IAH]_0$ remaining for side reactions. As discussed in previous text, high mobility of IAH and L101$^{\bullet}$ allows their interactions.

Under reaction conditions supporting β-scission, IAH can participate on reaction with PLA$^{\bullet}$ containing radical site at the end of chain. As $[IAH]_0$ increases and $[L101]_0$ is constant, end-chain grafting is responsible for increase of $[IAH]_{PLA}$ though molecular weight of PLA-g-IAH may decrease.

It can be concluded that at different $[IAH]_0$ and $[L101]_0$ different reactions predominate which has strong effect on grafting yield. Influence of different reaction parameters is summarized:

- low $[IAH]_0$ and low $[L101]_0$ – low grafting degree and low extent of side reactions; termination mainly via recombination of L101$^{\bullet}$ (Scheme 1, reaction 1a),
- low $[IAH]_0$ and high $[L101]_0$ – high concentration of PLA$^{\bullet}$, increase of grafting degree, termination mainly via recombination of L101$^{\bullet}$, PLA$^{\bullet}$-L101$^{\bullet}$ and PLA$^{\bullet}$-PLA$^{\bullet}$ interactions (Scheme 1, reactions 1a, 2a and 2b),
- high $[IAH]_0$ and low [L101] – high grafting degree and high amount of byproducts (low conversion); termination via L101$^{\bullet}$ recombination and PLA-g-IAH$^{\bullet}$-L101$^{\bullet}$ interactions (Scheme 1, reaction 1a and 3a),
- high $[IAH]_0$ and high [L101] – reaction between IAH and L101$^{\bullet}$ is favoured which limits grafting degree; termination via formation of low reactive IAH$^{\bullet}$ (Scheme 1, reaction 1b).

5.4.2 Reaction conditions affecting kinetics of grafting

As mentioned previously, radical reaction between PLA and IAH is a complex of reactions which proceed simultaneously. Fukuoka [42] described radical grafting of vinylsilane onto polyethylene as a complex of reactions which can be expressed for reaction between PLA and IAH by following equations:

$$L101 \xrightarrow{k_d} 2R^{\bullet} \tag{6a}$$

$$R^{\bullet} + PLA \xrightarrow{k_i} PLA^{\bullet} + RH \tag{6b}$$

$$PLA^{\bullet} + IAH \xrightarrow{k_g} PLA - g - IAH^{\bullet} \tag{6c}$$

$$PLA - g - IAH^{\bullet} + PLA \xrightarrow{k_{tr}} PLA - g - IAH + PLA^{\bullet} \tag{6d}$$

$$PLA^{\bullet} + PLA^{\bullet} \xrightarrow{k_t} PLA - PLA \tag{6e}$$

Proposed reaction complex includes decomposition of initiator generating L101$^{\bullet}$ (6a), formation of PLA$^{\bullet}$ by hydrogen abstraction from PLA backbone (6b), addition of IAH monomer onto active center formed on PLA chain (6c), radical transfer between PLA-g-IAH$^{\bullet}$ and PLA by hydrogen abstraction (6d) and coupling of PLA$^{\bullet}$ forming crosslinked chains (6e).

Elementary reaction expressed by Equation 6a–e can be written by kinetic equations as follow:

$$-\frac{d[L101]}{dt} = k_d \cdot [L101] \tag{7a}$$

$$\frac{d[R^{\bullet}]}{dt} = 2 \cdot f \cdot k_d \cdot [L101] - k_i \cdot [R^{\bullet}] \cdot [PLA] \tag{7b}$$

$$-\frac{d[IAH]}{dt} = k_g \cdot [PLA^{\bullet}] \cdot [IAH] \tag{7c}$$

$$\frac{d[PLA - IAH^{\bullet}]}{dt} = k_g \cdot [PLA^{\bullet}] \cdot [IAH] - k_{tr} \cdot [PLA - IAH^{\bullet}] \cdot [PLA] \tag{7d}$$

$$\frac{d[PLA^{\bullet}]}{dt} = k_i \cdot [R^{\bullet}] \cdot [PLA] - k_g \cdot [PLA^{\bullet}] \cdot [IAH] + k_{tr} \cdot [PLA - IAH^{\bullet}] \cdot [PLA] - k_t \cdot [PLA^{\bullet}]^2 \tag{7e}$$

In this reaction complex [L101] represents concentration of initiator, [R$^{\bullet}$] is concentration of primary radicals as a result of L101 thermal decomposition, *f* is the initiator efficiency, [IAH] is assigned to the concentration of monomer IAH, [PLA-IAH$^{\bullet}$] is concentration of lactic unit with grafted IAH, [PLA] and [PLA$^{\bullet}$] represent concentrations of lactic units in the polymer chain and its radicals, respectively.

Quasi-steady-state approximation can be used for study of kinetics of chemical reaction where free radicals and other unstable molecules have very short time of existence. Quasi-steady-state can be derived from Equations 7b, d, e and expressed using Equations 8 and 9, whereas their incorporation into the Equation 6c provides a rate Equation 10:

$$k_i \cdot [R^{\bullet}] = 2 \cdot f \cdot k_d \cdot \frac{[L101]}{[PLA]} \quad (8)$$

$$2 \cdot f \cdot k_d \cdot [L101] = k_t \cdot [PLA^{\bullet}]^2 \quad (9)$$

$$\frac{d\alpha}{dt} = K \cdot (1 - \alpha) \cdot [L101]^{1/2} \quad (10)$$

where α represents reaction conversion and K is apparent rate constant given by Equation 11:

$$K = \sqrt{\frac{2 \cdot f \cdot k_d \cdot k_g^2}{k_t}} \quad (11)$$

Reaction conditions applied for kinetic experiments are summarized in Table 6. Regarding previous results, reaction between PLA and low amount of both IAH and L101 exhibit limited extent of side reactions and provide sufficient grafting yield. Therefore, PLA-g-IAH was prepared at constant $[IAH]_0$ (0.5 wt %) and different $[L101]_0$ (0.1, 0.5 and 1 wt %). Influence of various reaction temperature (170, 190 and 210 °C) on kinetic parameters was evaluated.

Plot in Figure 14 shows the relationship between reaction conversion and reaction time determined for reaction between PLA and IAH initiated by various $[L101]_0$. After 10 minutes the lowest conversion was reached for reaction between PLA and IAH at 170 °C except of the reaction system with the lowest $[L101]_0$ (0.1 wt %). This reaction system exhibited lowest conversion at 210 °C where the highest concentration of $L101^{\bullet}$ is presented in reaction system in gradient of time. At these conditions, low concentration of initiator is available for grafting reaction and $L101^{\bullet}$ are preferably consumed via theire recombination and interactions with $PLA^{\bullet}$. On the other hand, at higher $[L101]_0$ (0.5 and 1 wt %) the lowest conversion was reached at reaction temperature of 170 °C. This is due to shape of exponential plot between $[L101]/[L101]_0$ and reaction time. After 10 minutes of reaction period, certain amount of unreacted initiator (~10 %) still remains in reaction system (black curve in Figure 7, chapter 4.2). This fact leads to slight increase of conversion with increase of reaction time and incomplete grafting reaction with unreacted IAH.

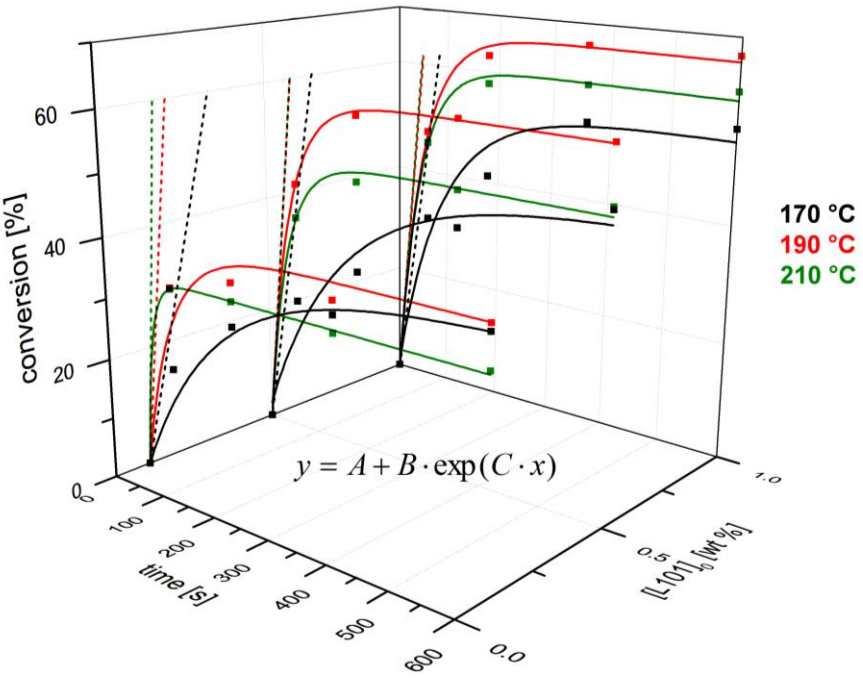

Figure 14. Kinetic data - relationship between reaction conversion and reaction time fitted by simple exponential function (solid curves), initial grafting rate R_{gi} (dashed curves) derived from linear part of exponential function; kinetic data for samples 0.5-x where x = $[L101]_0$ = 0.1–1 wt %; T_r = 170, 190 and 210 °C.

Apparent rate constant K expressed by Equation 11 was determined as a slope of semi-logarithmic plot between (1-α) and ($[L101]_0^{1/2}$ - $[L101]^{1/2}$) giving Equation 12:

$$\ln\left(1-\alpha\right) = -\frac{2\cdot K}{k_d}\cdot\left(\left[L101\right]_0^{1/2} - \left[L101\right]^{1/2}\right) \tag{12}$$

where $[L101]_0^{1/2}$ represents square root of initial concentration of L101, k_d equals to decomposition rate constant of L101 and $[L101]^{1/2}$ is square root of actual concentration of L101 calculated by Equation 13. Derived rate constants K are shown in Table 8

$$\left[L101\right] = \left[L101\right]_0 \cdot \exp\left(-k_d \cdot t\right) \tag{13}$$

Rate constant K expressed by Equation 11 contains rate constants of individual reactions including decomposition of initiator (k_d), grafting (k_g) and termination (k_t). Using known values of K and k_d, it was able to express k_g^2/k_t (Table 8) whereas relation between its logarithmic form $\ln(k_g^2/k_t)$ and 1/T is reflected in Figure 14c. Linear regression provides slope which is relevant to E_a/R giving value of E_a. Plot in Figure 14c suggests its activation energy to be negative, interpreting that the addition reaction is faster or the termination reaction is slower at lower temperature in the elementary reactions. It implies that mobility of macroradicals would be limited at lower temperature and termination reactions among them hardly occur.

Table 8. Kinetic parameters obtained from experimental data; PLA-g-IAH samples 0.5-x where x = $[L101]_0$ = 0.1–1 wt %, 170–210 °C.

sample	T_r [°C]	K [10^6]	$k_g/k_t^{1/2}$ [10^3]	E_a [kJ·mol^{-1}]
0.5-0.1		0.6057	5.98	-183.0
0.5-0.5	170	0.3555	3.51	-173.9
0.5-1		0.3283	3.24	-170.9
0.5-0.1		0.4316	1.69	-201.0
0.5-0.5	190	0.3506	1.37	-189.0
0.5-1		0.3003	1.18	-186.5
0.5-0.1		0.3402	0.57	-218.4
0.5-0.5	210	0.2385	0.40	-207.1
0.5-1		0.2317	0.39	-203.4

5.5 IAH homopolymerization during radical grafting

5.5.1 Simulation of IAH radical polymerization in melt

Supposed structure of PLA-g-IAH was evaluated using FTIR with respect to reaction mechanism in Scheme 1. Except of undesired reaction discussed in this work, homopolymerization of IAH occurs under certain conditions and is theoretically predicted in Scheme 1, reaction 1aa. Many researches neglect homopolymerization of cyclic anhydrides (e.g. maleic anhydride, citraconic anhydride, etc.)during functionalization of polymers. These assumptions are based on the value of ceiling polymerization temperature (T_c) determined for IAH solution polymerization [43]–[44]. Nevertheless, this prediction is not usually experimentally proved in the literature. Therefore, reaction between IAH and L101 at different IAH/L101 molar ratio was achieved in the glass tube heated at 190 °C for 6 min. Reaction products were analyzed by FTIR analysis and measured FTIR spectra are presented in Figure 15. Samples 2.59–259.11 represent IAH/L101 molar ratios used for radical grafting according to reaction conditions summarized in Table 7. FTIR spectrum of IAH exhibits absorption bands at 1850, 1760, 1665 and 930 cm^{-1} which are assigned to C=O (stretching vibration), C=O (stretching vibration), CH_2=C< (stretching vibration) and CH_2=C< (out plane deformation), respectively [45]. On the other hand, FTIR spectrum of p(IAH) prepared by low-temperature solution polymerization exhibits slight shifting of C=O absorption bands from 1850 and 1760 cm^{-1} to 1860 and 1775 cm^{-1}, respectively. Low intensity of shifted bands may reflect low reaction conversion which was reported by Otsu and Yang [46] who discussed results of radical IAH polymerization at different reaction temperatures and initiators. In consistence with results presented by Otsu and Yang, relatively low polymerization degree can be expected due to low reactivity of secondary radicals generated from thermal decomposition of L101.

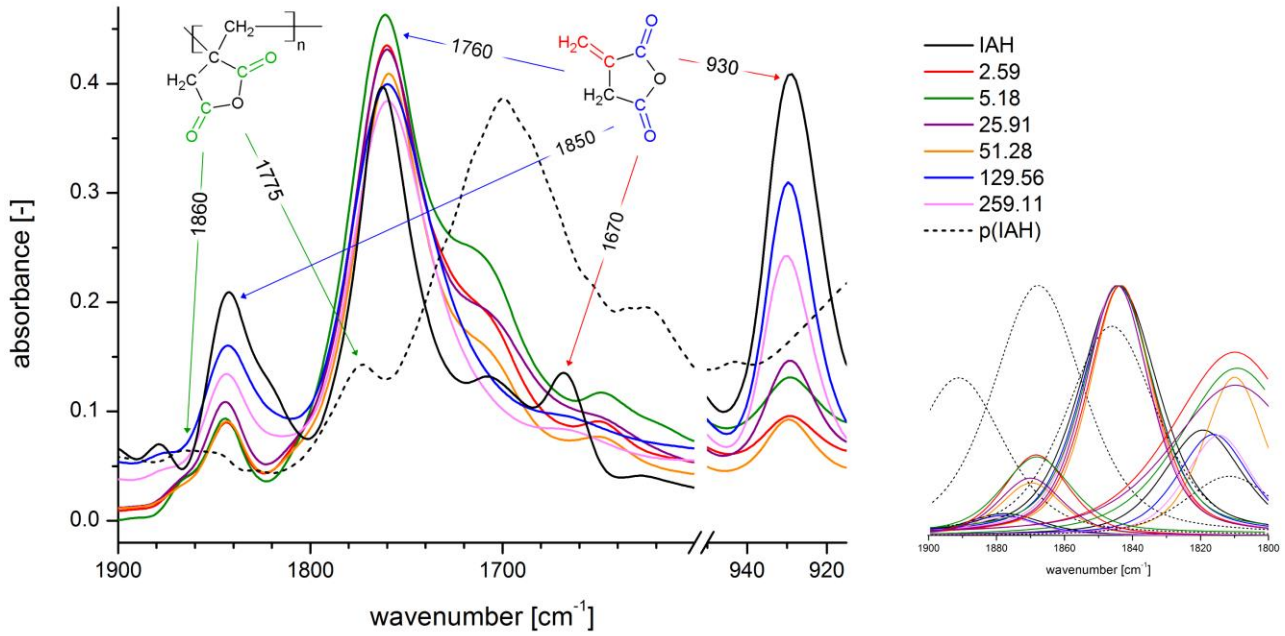

Figure 15. FTIR spectra of IAH, p(IAH) prepared by solution polymerization of IAH and products of radical reaction in melt between IAH and L101at different IAH/L101 molar ratio and 190 °C; FTIR spectra normalized to intensity of C=O absorption band centered at 1760 cm^{-1}.

In the case of p(IAH), absorption bands typical for CH_2=C< fragment (1665 and 930 cm^{-1}) disappeared due to consumption of double bonds during IAH polymerization. Integral intensity of absorption band at 930 cm^{-1} decreases as IAH/L101 molar ratio decreases. It corresponds to the higher extent of IAH-L101$^{\bullet}$ interactions and decreasing concentration of CH_2=C bonds due to formation of p(IAH) macromolecules. It can be expected that at high concentration of L101, reaction between L101$^{\bullet}$ and IAH occur with higher probability. Consequently, absorption band at 1665 cm^{-1} disappeared due to mentioned preferable reactions. However, weak peak at 1665 cm^{-1} was observed for for samples 129.56 and 259.11 due to low extent of IAH-L101$^{\bullet}$ interactions as well as low polymerization yield.

Further difference in FTIR spectra was observed in wavenumber range 1850–1860 cm^{-1} which is typical for C=O stretching vibrations of IAH and p(IAH) detected at lower and higher wavenumber, respectively. FTIR spectra of samples 2.59, 5.18, 25.91 and 51.28 contain absorption band at 1860 cm^{-1} which suggests presence of p(IAH). On the other hand, only weak shoulder of mentioned absorption band was observed for samples with high IAH/L101 molar ratio (129.56 and 259.11). Consequently, IAH homopolymerization seems to be supressed at high IAH/L101 ratio due to low concentration of L101$^{\bullet}$ and high degree of termination reactions.

FTIR spectra in Figure 15 were deconvoluted in order to detect overlapped absorption bands characteristic for C=O groups in wavenumber range 1900–1800 cm^{-1}. Absorption band centered at 1840 cm^{-1} was split into three and four individual peaks for samples 2.59–259.11 and p(IAH), respectively. Absorption band at 1845 cm^{-1} was detected for all samples. With regard to previous text, this absorption band was attributed to C=O stretching vibrations of anhydride ring as a single molecule. On the other hand, samples 2.59, 5.18, 25.91, 51.28 and p(IAH) exhibit

absorption band shifted to higher frequency of C=O stretching with maximum at 1870 cm^{-1}. This fact is consistent with formation of p(IAH). C=O stretch vibrations of samples 129.56 and 259.11 are shifted to 1875 cm^{-1} which may indicate polymeric chains with higher amount of IAH units incorporated in p(IAH) chain. Unfortunately, relatively low intensity of this absorption band predicts low concentration of p(IAH) chains with high polymerization degree. This is in agreement with position of absorption band at around 1810 cm^{-1} which is characteristic for C–H vibrations of vinyl hydrocarbon compounds. Samples 129.56 and 259.11 contain peak centered at 1816 and 1815 cm^{-1}, respectively. On the other hand, samples with lower IAH/L101 molar ratio exhibit peak maximum at 1810 cm^{-1} which is closer to p(IAH). Consequently, lower frequency of C=C stretch could reflect C–C single bonds presented in p(IAH).

Figure 16 represents TGA experimental data given by plot between weight loss and temperature. It is clear that IAH decomposes in two steps. First decomposition step is situated in the temperature range 60–180 °C with T_{max} 150 °C and can be assigned to the release of water from hydrated IAH and its subsequent decomposition. Second decomposition step observed in the range 180–220 °C could reflect self-induced polymerization of IAH. This prediction is inspired by results of Katime, Madoz and Velada [47] who proved self-induced polymerization of itaconate esters without using AIBN. In the case of IAH, approximately 2 wt % of carbonaceous char residue remained at 600 °C. On the other hand, TGA curve of p(IAH) consists of five distinct decomposition steps with T_{max} ~70, 160, 190, 290 and 400 °C. At 600 °C ~27.6 wt % of carbonaceous char residue remained which is typical for p(IAH) and will be also discussed in chapter 5.5.2.

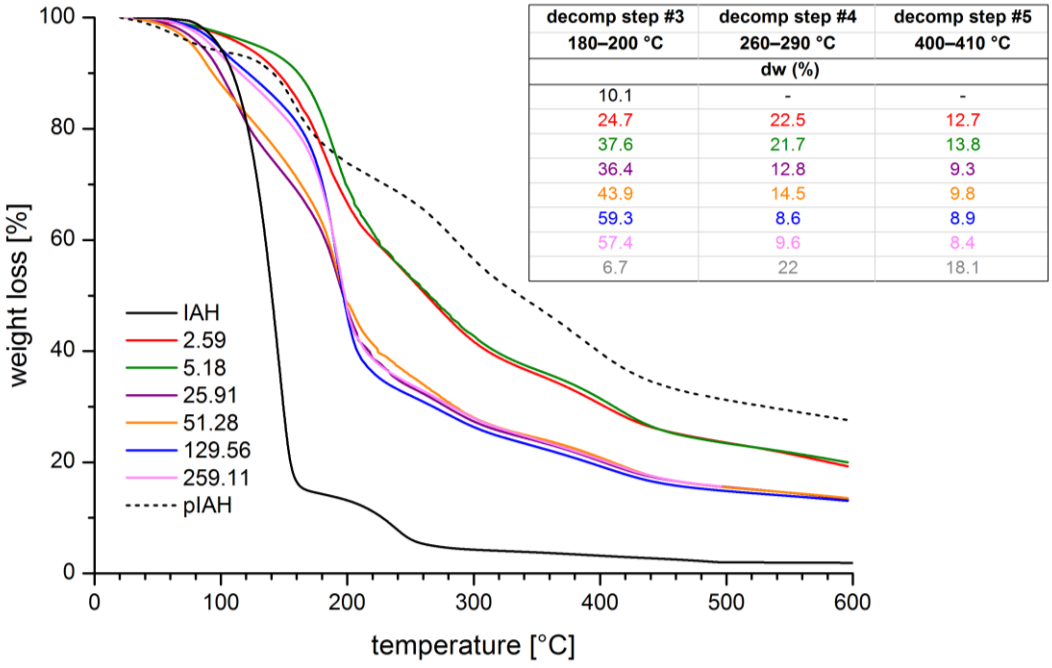

Figure 16. TGA thermogram of samples prepared by reaction between IAH and L101 at 190 °C and different IAH/L101 molar ratio.

Samples 2.59–259.11 exhibit similar shape of TGA curves which consist of four decomposition steps. Weight losses of individual decomposed fractions are included in Figure 16. It was expected that conversion of IAH polymerization will be low and this assumption was proved for samples 25.91–259.11. These samples contained ~13 wt % of char residue which is lower than for both p(IAH) and samples 2.59 and 5.18. As discussed previously, IAH homopolymerization under proposed reaction conditions is complicated due to several factors, such as low thermal stability of IAH, isomerization into more stable CAH or favoured coupling of radical species. Therefore, it can be predicted that solution polymerization reaches higher conversion due no IAH isomerization, low concentration of free radicals and limited degradation. This was proved by higher amount of char residue of p(IAH) prepared by solution polymerization compared to samples 2.59–259.11 prepared via reaction in melt. High $[L101]_0$ applied for sample 2.59 leads to higher extent of IAH-L101$^{\bullet}$ interactions and formation of p(IAH) with higher polydispersity. Increasing IAH/L101 molar ratio could increase molecular weight of p(IAH). However, for example thermal stability of sample 259.11 is similar to the thermal stability of sample 5.18. This fact is probably caused by allylic hydrogen situated in IAH that can act as a chain transfer agent in radical polymerization which limits molecular weight of p(IAH [48] In addition, chain transfer is energetically demanding process which is favoured at elevated temperatures.

5.5.2 IAH polymerization during grafting reaction

As discussed above, concentration of reaction compounds influences many reaction markers, such as grafting degree or extent of side reactions. Byproducts can be detected according to different thermal stability compared to PLA matrix. Due to low concentration of byproducts generated during grafting process, extraction of these fractions was necessary. As discussed in previous chapter, the yield of IAH polymerization increases with increasing $[L101]_0$ due to more preferable reaction between L101$^{\bullet}$ and PLA backbone. Therefore, extraction was achieved for samples prepared by grafting reaction with different $[IAH]_0$ (0.5, 1, 5 and 10 wt %) and constant $[L101]_0$ (2 wt %).

Thermal stability of prepared extracts is shown in Figure 17. Extract of neat PLA exhibits two decomposition steps with T_{max} ~120 and ~350 °C. First decomposition step is assigned to release of residual moisture and residual monomer (lactide) whereas the second major decomposition step reflects decomposition of PLA matrix. Sample 0.5-2 and 1-2 exhibits two distinct degradation steps with T_{max} ~200 and ~340 °C. Degradation step at lower temperature can be assigned to combination of release of water from anhydride ring and beginning degradation of IAH and p(IAH). With respect to TGA curve of neat PLA, upper degradation temperature can be assigned to degradation of PLA. No char residue remained at 500 °C. On the other hand, TGA curve of sample 5-2 and 10-2 consists of three decomposition steps with T_{max} ~180, ~260 and ~350 °C. In addition, 4.6 and 8.3 wt % of carbonaceous char residue remained at 500 °C for sample ex 5-2 and ex 10-2, respectively. The carbonaceous char is expected to be condensed crosslinked structure formed by decarboxylation and decarbonylation of the anhydride ring [49].

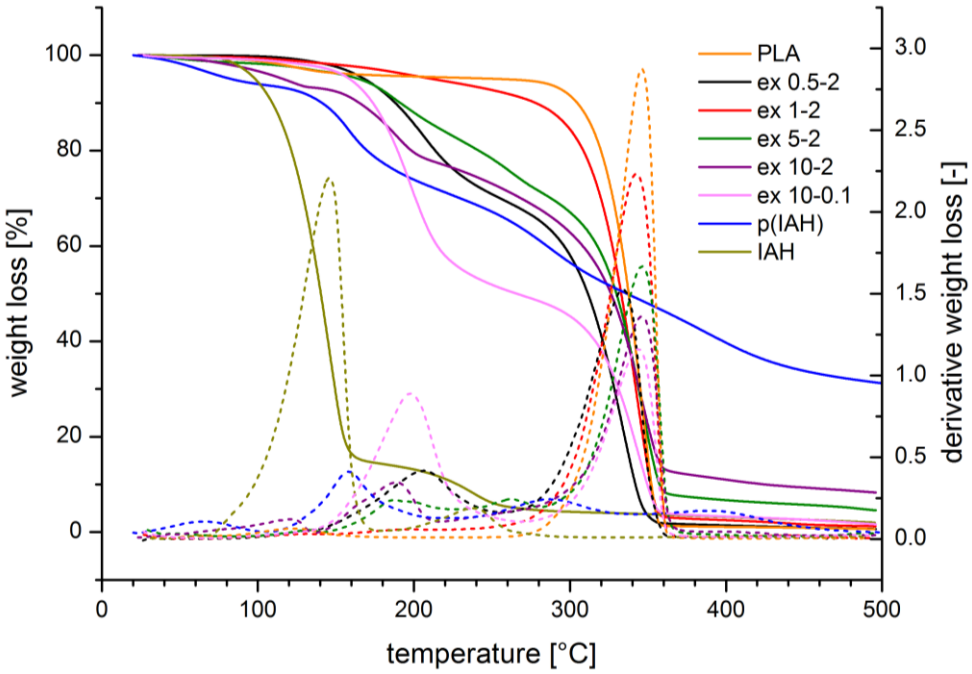

Figure 17. Thermal stability of neat PLA, IAH, p(IAH) and samples prepared by extraction of PLA-g-IAH in acetone.

Thermal stability of extracted samples were compared to those obtained for p(IAH) prepared according to method described in chapter 4.2. Four decomposition steps were observed at ~60, ~160, ~290 and ~390 °C and the amount of char remaining was 27.6 wt % which is in agreement with TGA data described by Shang et al. [50] who synthesized and characterized itaconic anhydride and stearyl methacrylate copolymers.

TGA curves of samples ex 5-2 and ex 10-2 are similar to p(IAH) in the temperature range 220–300 °C. Third decomposition step of p(IAH) begins at ~240 °C which is similar to sample ex 5-2 and ex 10-2. Sample ex 5-2 exhibits third decomposition step which is clerly separated from the decomposition of PLA matrix centered at ~350 °C. On the other hand, sample ex 10-2 exhibits continuous degradation from ~220 °C up to ~280 °C where above this temperature PLA begins degrading. Broad range of decomposition temperature reflects gradual weight loss suggesting higher polydispersity of p(IAH) extracted from the sample ex 10-2 compared to the sample ex 5-2.

Theoretically, general polymerization requires high IAH/L101 ratio in order to prepare polymer with high molecular weight. Therefore, thermal stability of extracted samples ex 10-0.1 and ex 10-2 was compared in order to prove this theory. As shown in Figure 17, both samples are decomposed in two major decomposition steps. First decomposition step is centered at ~200 °C, second one is centered at ~350 °C. Furthermore, sample 10-2 exhibit significant weight loss above 220 °C which was desribed above as a result of p(IAH) decomposition. Obtained results prove assumption that most of L101$^{\bullet}$ are consumed via reaction with PLA or via their recombination. Similar δ of IAH and L101 allow IAH homopolymerization at $[IAH]_0$ and $[L101]_0$.

5.5.3 Reaction conditions supporting self-induced reactions of IAH

High reactivity of IAH allows its application for reactive modification of polymers due to several factors. First, reactivity of –CO–O–CO– anhydride group allows subsequent reactions with different compounds such as amines. These amines can be derived from natural sources (e.g. proteins) or can be synthetically prepared. This fact enlarges applicability of PLA modified with IAH. Second, higher reactivity of IAH can be predicted due to different possition of C=C double bond of IAH compared to MAH. This may positively affect grafting process. On the other hand, IAH polymerization could become more favourable during functionalization.

Some studies propose that IAH isomerizes to citraconic anhydride (CAH) at the temperature above 100 °C [51]. Therefore, most of functionalization procedures are achieved in solution at low temperature to avoid IAH isomerization. Since exact temperature of IAH-CAH isomerization was not found in the literature, structure analysis was achieved for IAH which was treated under different temperature (80–180 °C) for 6 min. Reaction temperature was chosen with respect to the melting temperature of IAH (66–68 °C) and residence time was the same as used for grafting reaction.

Figure 18 represents FTIR spectra of analyzed samples in the range of 950–750 cm^{-1} as well as structure of both IAH and CAH. Samples prepared at the temperature above 120 °C exhibit weak absorption band at around 870 cm^{-1} which can be attributed to –C=CH– functional group included in the CAH structure. Peaks at around 910 cm^{-1} and 780 cm^{-1} can be assigned to vibrations of $–C=CH_2$ functional group characteristic for IAH structure [52].

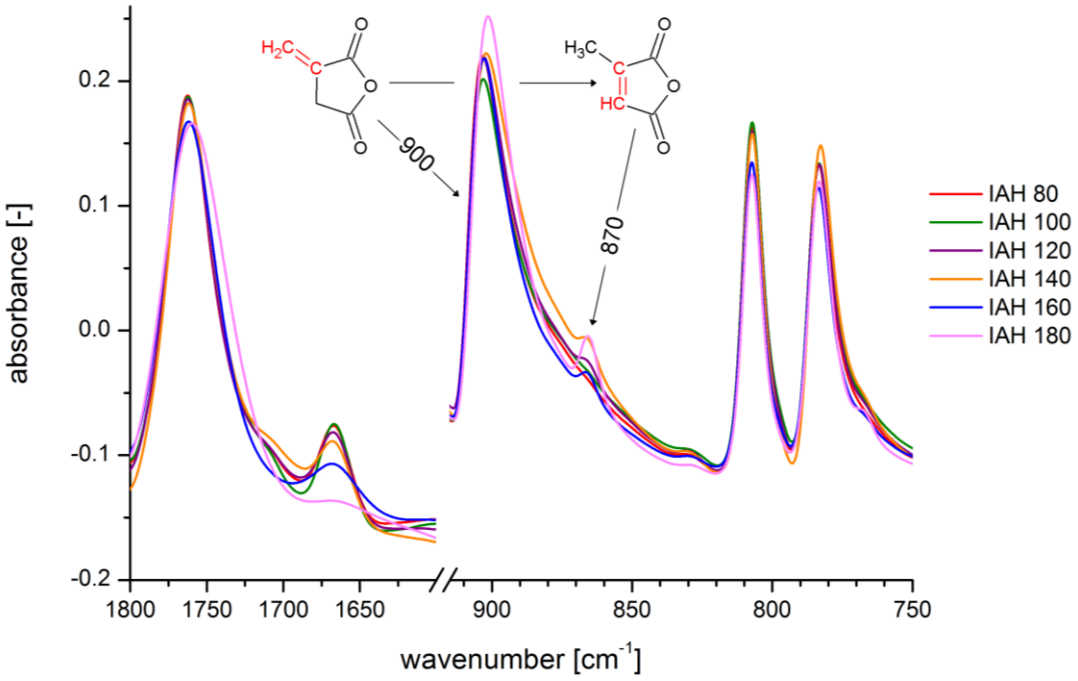

Figure 18. FTIR spectrum for IAH heated at different temperature.

IAH isomerization was also observed on both DSC and DTA thermograms shown in Figure 19a. DSC curve exhibits sharp endothermic peak at around 70 °C which relates to the melting of IAH. Except of melting, exothermic peak with maximum at ~130 °C was detected. It can be attributed to the isomerization from IAH to citranonic anhydride (CAH) [51] which was proved by FTIR analysis. Exothermic peak located at ~170 °C could be assigned to self induced polymerization. This hypothesis is based on the results presented by Katime, Madoz and Velada [47] who described self induced polymerization of itaconate derivates. In this research, polymerization temperature range was evaluated for different itaconate esters with and without using AIBN. Unlike diphenyl itaconate, both dibenzyl itaconate and di-2-phenylethyl itaconate polymerized without AIBN. It was explained by the sterric effect of side groups and loss of conjugation which corresponds to monomer-polymer transformation. Polymerization of unsaturated bonds consists of the opening of one double bond and formation of two single bonds. Accordingly, reaction heat was calculated as a difference between reaction heat of disruption of C=C double bond (608.8 $kJ \cdot mol^{-1}$) and formation of C-C bond (702.9 $kJ \cdot mol^{-1}$) equals to 94.1 $kJ \cdot mol^{-1}$ [47]. From the heat of reaction derived from DSC curve in Figure 19a (22.5 $J \cdot g^{-1} \approx 2.5\ kJ \cdot mol^{-1}$) it can be assumed that self-induced polymerization of IAH becomes very difficult. This fact is also supported by isomerization IAH-CAH whereas less reactive CAH limits polymerization yield. Degradation of IAH was detected on DTA thermogram as an endothermic peak (red curve, T_{max} ~150 °C) and degradation products were detected in FTIR spectra. Therefore, it can be concluded that IAH degradation and self-induced polymerization proceed simultaneously.

TGA thermograms in Figure 19b proved self-induced IAH polymerization. Decomposition profile of samples IAH 80–140 is similar to the decomposition profile of neat IAH. Main decomposition step was detected at ~140–160 °C. Second minor decomposition step was observed at ~230–240 °C. Approximately 1–2 wt % of char residue remained at 500 °C for those samples. On the other hand, samples IAH 160 and IAH 180 decompose differently whereas second minor decomposition step was not so clear and char residue increased up to 4 wt %. Change of thermal stability and higher content of char residue can be attributed to higher content of polymerized IAH.

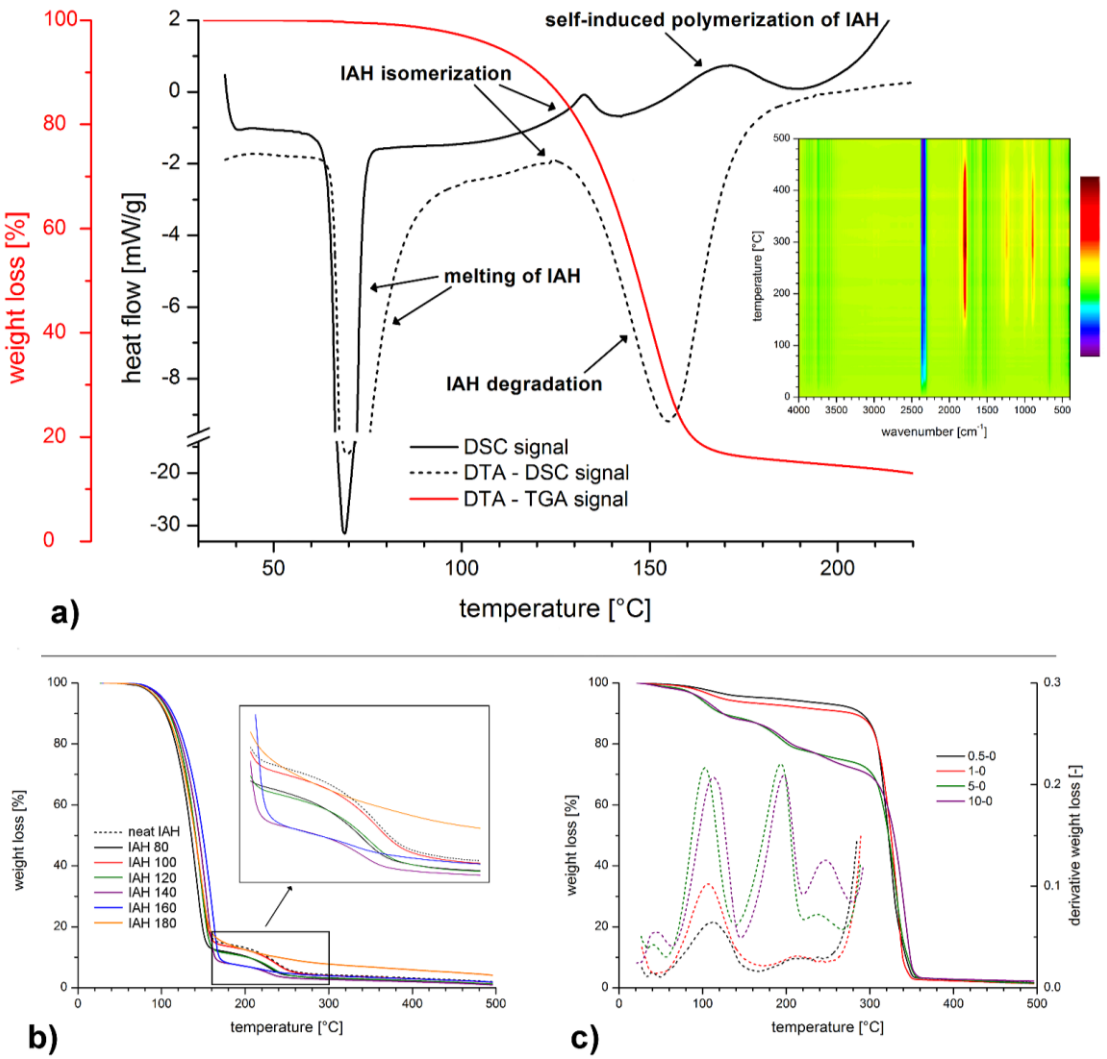

Figure 19. Self-induced polymerization of IAH investigated "in situ" by DSC and DTA (a); decomposition of IAH treated at different temperatures (b); thermal stability of fractions extracted from PLA/IAH blends (c).

Only a few authors deal with thermal stability of IAH and IAH based polymers for last few decades. For example, Rice and Murphy [45] briefly described isothermal decomposition of IAH where methylacetylene, allene, carbon monooxide and carbon dioxide were detected as decomposition products. Compared to this, proposed thesis illustrates IAH decomposition upon temeprature ramp. As mentioned previously, IAH isomerizes at temperature above 120 °C. Major decomposition step can be assigned to decomposition of IAH whereas IAH probably isomerizes while it was being evaporated. Second decomposition step begins at ~170 °C probably as a result of formation of more stable dimer and/or oligomer form of IAH. It can be assumed that both self-induced and L101-initiated IAH polymerization can occur under reaction conditions used for radical grafting of PLA.

Self-induced IAH polymerization was considered to be possible at temperature above 160 °C. Previous experiments were achieved without presence of any other compounds such as polymer

matrix. Therefore, PLA/IAH blends were prepared at 190 °C and thermal stability of acetone soluble fractions was evaluated using TGA analysis. Decomposition profile of thus prepared samples is given in Figure 19c. Fractions extracted from PLA/IAH blends with low $[IAH]_0$ (samples 0.5-0 and 1-0) contain low amount of low-molecular fractions composed of IAH oligomers. It is probably caused by combination of several factors. First, high reaction temperature and low $[IAH]_0$ enhance IAH degradation and limit IAH-IAH interactions. Second, low concentration and high melt viscosity limit IAH-IAH interactions due to intensive homogenization during processing. On the other hand, samples ex 5-0 and ex 10-0 contain significantly higher amount of IAH oligomers. At high $[IAH]_0$, IAH molecules can partially agregate although intensive homogenization was applied. In this case, IAH polymerization can reach higher yield.

As mentioned above, Shang et al. [50] observed thermal decomposition of p(IAH) beginning at ~170 °C. However, authors did not describe individual fractions decomposed during heat ramp. Therefore, thermal decomposition of IAH was studied using TGA achieved at different heating rate (2–50 °C/min.) and obtained data are shown in Figure 20. Two distinct decomposition steps were detected which is in consistence with previous results. Major decomposition step is assigned to decomposition of IAH or its isomeric form CAH which can be generated simultaneously with decomposition of IAH. Further decomposition continues at temperature above 150 °C while onset temperature depends on the haeting rate. Shang et al. [50] reflect this decomposition step as a consequence of radical polymerization of IAH. However, experimental data in Figure 20 were obtained for IAH without initiator. Therefore, second decomposition step may reflect decomposition of IAH dimers or oligomers.

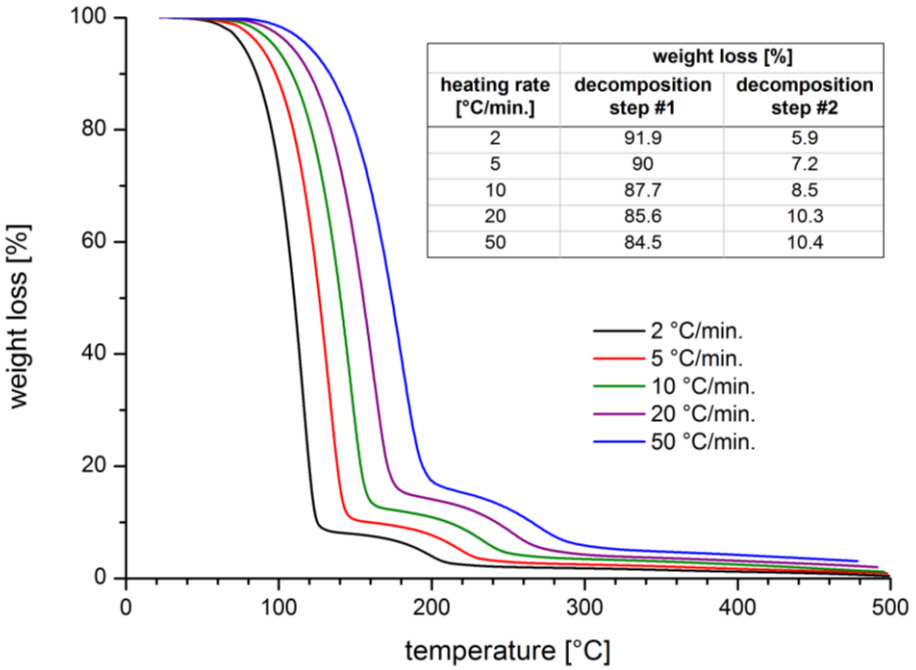

	weight loss [%]	
heating rate [°C/min.]	decomposition step #1	decomposition step #2
2	91.9	5.9
5	90	7.2
10	87.7	8.5
20	85.6	10.3
50	84.5	10.4

Figure 20. TGA thermogram of IAH decomposed at different heating rate.

Increase of T_{max} of both decomposed fractions relates to slower response of TGA signal due to higher heating rate. Figure 20 includes values of weight losses of both decomposed fractions. It can be concluded that higher heating rate results in lower amount of decomposed IAH while amount of IAH dimers/oligomers increases. Low heating rate gives greater yield of IAH degradation whereas high heating rate (i.e. 20 °C/min.) inhibits IAH degradation and higher amount of IAH is available for coupling reactions at higher temperature.

5.6 Effect of reactive modification on PLA biodegradability

The influence of reaction conditions on PLA-g-IAH structure and relating degradation rate was investigated during long-term biodegradation test for 12 weeks. The effect of accumulated degradation products on pH values and degradation profile of PLA-g-IAH prepared at various $[IAH]_0$ (0.5, 1 and 5 wt %) and $[L101]_0$ (0.1, 0.5 and 1 wt %) was investigated. Neat PLA was used as a reference sample to evaluate the effect of grafted IAH on biodegradation.

Figure 21 represents degradation profile of PLA-g-IAH samples. As PLA-g-IAH was incubated in distilled water, pH of medium decreased with increasing time. Generally, decrease of pH can be assigned to higher concentration of degradation products. The degradation of PLA and PLA-g-IAH consist of four consecutive steps: hydration, initial degradation, further degradation and solubilization [53].

Three degradation steps can be observed in Figure 21. First part of degradation process is characterized by decrease of pH from 5.1 to 5.0 for neat PLA and from 5.7 to 3.7 for PLA-g-IAH. During this degradation medium penetrates into the polymer matrix without chain cleavage. It is clear, that hydration of neat PLA occured for two weeks while first degradation phase of PLA-g-IAH occured within one week. Furthermore, first degradation phase is characterized by slight decline of pH value which was observed for neat PLA while PLA-g-IAH exhibited strong decline of pH value within first week. This can be attributed to PLA-g-IAH's higher content of amorphous phase which enhances faster penetration of aqueous medium into PLA. In addition, first phase can be overlapped by second phase in the case of PLA-g-IAH. With respect to the concentration of reaction compounds, increase of both $[IAH]_0$ and $[L101]_0$ results in more intensive first hydration stage due to higher content of amorphous phase, higher grafting degree and reduced chain mobility. This is mostly evident for samples 5-1 which exhibits pH value drop from 5.5 to 3.8 within one week.

Second phase of PLA degradation exhibits increasing rate of degradation which is observed by significant decline of pH value. During this phase, ester bond are hydrolyzed and increasing concentration of carboxyl groups accelerates hydrolysis. This phase was observed from second to fourth week for neat PLA and from first to fourth week for PLA-g-IAH. In this degradation period, pH value dropped from 5.0 to 4.0 and from 5.2 to 3.5 for neat PLA and PLA-g-IAH, respectively. In the case of PLA-g-IAH, presence of grafted IAH supports hydrolysis of ester bond. Anhydride groups in PLA-g-IAH hydrolyze to form carboxyl groups which drop pH values of aqueous medium. This effect could be desired in certain medical applications which require fast and controlled degradation of applied material with intensive drug release.

In the third phase, pH decreases gradually from 4.0 to 3.0 and from 3.5 to 2.7 for neat PLA and PLA-g-IAH, respectively. In this phase, the rate of degradation declines and after eleven weeks the pH values reach plateau due to the slowdown of polymer degradation [54].

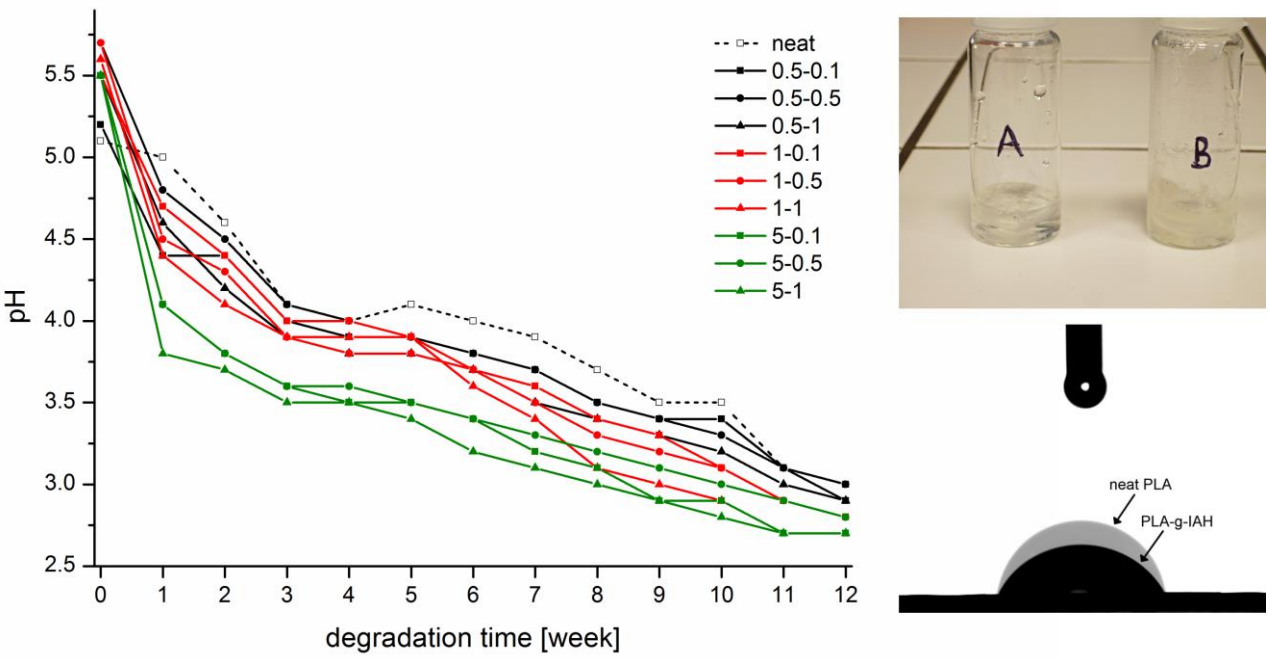

Figure 21. Time dependent pH change of aqueous media during the biodegradation of PLA and PLA-g-IAH at 37±0.1 °C; $[IAH]_0$ = 0.5, 1 and 5 wt %, $[L101]_0$ = 0.1, 0.5 and 1 wt %; sample before (A) and after (B) biodegradation test; contact angle of PLA and PLA-g-IAH.

As discussed previously, grafted IAH enhances biodegradability of modified PLA. Contact angle measurement proved enhanced hydrophilicity of PLA-g-IAH detected by decrease of contact angle compared to neat PLA. Improved hydrophilicity supports degradation of PLA-g-IAH as well as lower crystallinity.

5.7 Change of thermal properties due to radical grafting

5.7.1 PLA-g-IAH structure detected by change of thermal properties

Relation between structure of modified PLA and thermal properties was interpreted using DSC analysis. DSC thermograms were obtained for purified PLA-g-IAH prepared at different $[IAH]_0$ and $[L101]_0$. Data obtained from the second heating cycle are presented in order to avoid the effect of thermal history. Absence of exothermic peak located above melting of PLA and endothermic peak of IAH melting (m.p. 60–70 °C) suggests complete grafting reaction with no reactants residue and succesful removing IAH from raw samples, respectively.

DSC curves obtained for x-0.1 samples (x = $[IAH]_0$ = 0.5–10 wt %) are given in Figure 22. The influence of PLA-g-IAH structure on characteristic phase transitions was observed. For all samples glass transition temperature T_g, cold crystallization temperature T_{cc} and melting temperature T_m were observed at around 50, 100 and 150 °C, respectively. For all PLA-g-IAH samples, lower T_g was observed as a result of change of segmental mobility of polymer chains compared to unprocessed PLA (T_g = 52.7 °C). As shown in Figure 22, relationship between $[IAH]_0$ and T_g of PLA-g-IAH is not clear. However, enhanced chain mobility resulted in decrease of T_g due to grafting of bulky anhydride ring. Similar results were discussed by Hwang et al. [27] who studied physical and mechanical properties of PLA grafted with maleic anhydride MAH (PLA-g-MAH). In this study T_g of PLA-g-MAH decreased as MAH content increased.

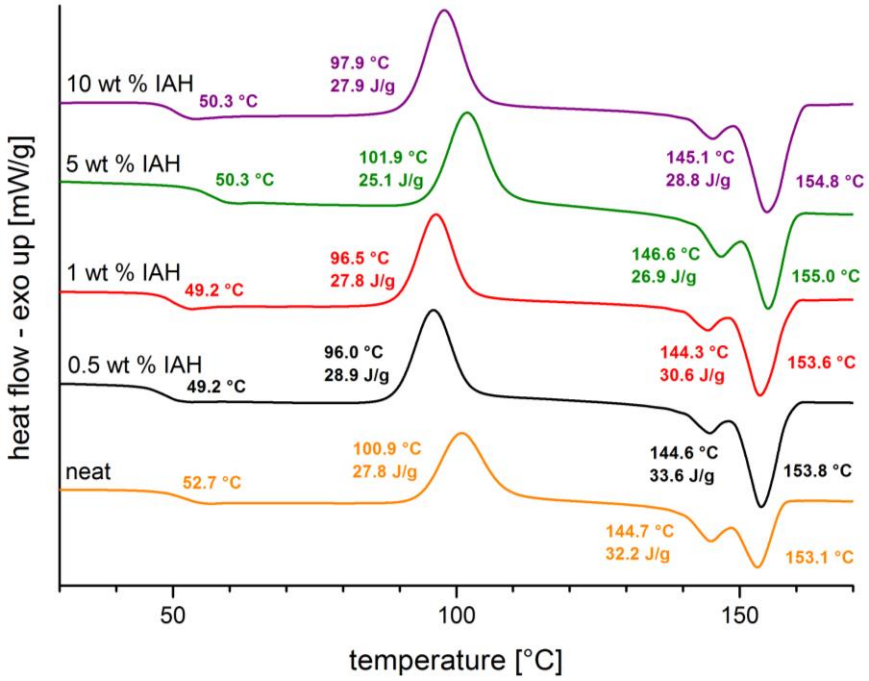

Figure 22. DSC thermograms of neat PLA and purified PLA-g-IAH with constant $[L101]_0$ (0.5 wt %) and different $[IAH]_0$; 2nd heating cycle.

DCS curve recorded for neat PLA contains exothermic peak attributed to cold crystallization at 100.9 °C which reflects organization of PLA structure upon heating cycle. PLA-g-IAH exhibits lower T_{cc} compared to neat PLA whereas T_{cc} increases with increasing $[IAH]_0$. Lower T_{cc} of PLA-g-IAH may suggest decrease of molecular weight. According to this hypothesis, PLA-g-IAH chains with lower molar mass can be oriented at lower temperature compared to PLA chains with greater molar mass which require higher temperature to be oriented. Two endothermic peaks at around 150 °C can be attributed to the melting of two different phase structures. Peak at lower temperature relates to α' phase and the second peak corresponds with α phase [55]. These two crystal modifications have a similar chain packing with 10_3 helix conformation and orthorhombic unit cell [56].

Degree of crystallinity of PLA-g-IAH was calculated according to Equation 5 in chapter 4.3. Degree of crystallinity of PLA-g-IAH was found to be lower compared to neat PLA as a result of

irregular PLA-g-IAH due to both IAH grafted on PLA backbone and side reactions such as branching or β-scission.

5.7.2 Thermal stability of modified PLA

Experiments investigated radical grafting of PLA "in situ" proved existence and degradation of byproducts generated simultaneously with main reaction. These byproducts were also detectede in PLA-g-IAH prepared in internal mixer due to different thermal stability. Figure 23 illustrates thermal stability of selected PLA-g-IAH samples prepared with 0.5 and 5 wt % IAH and 0.1–2 wt % L101. All tested grafted PLA had a lower thermal stability compared to neat PLA. The slight decrease in thermal stability supports earlier observations regarding a decrease in crystallinity. With regard to previous results, decrease of thermal stability can be relevant to decrease of molecular mass of functionalized PLA as a result of chain scission during radical grafting.

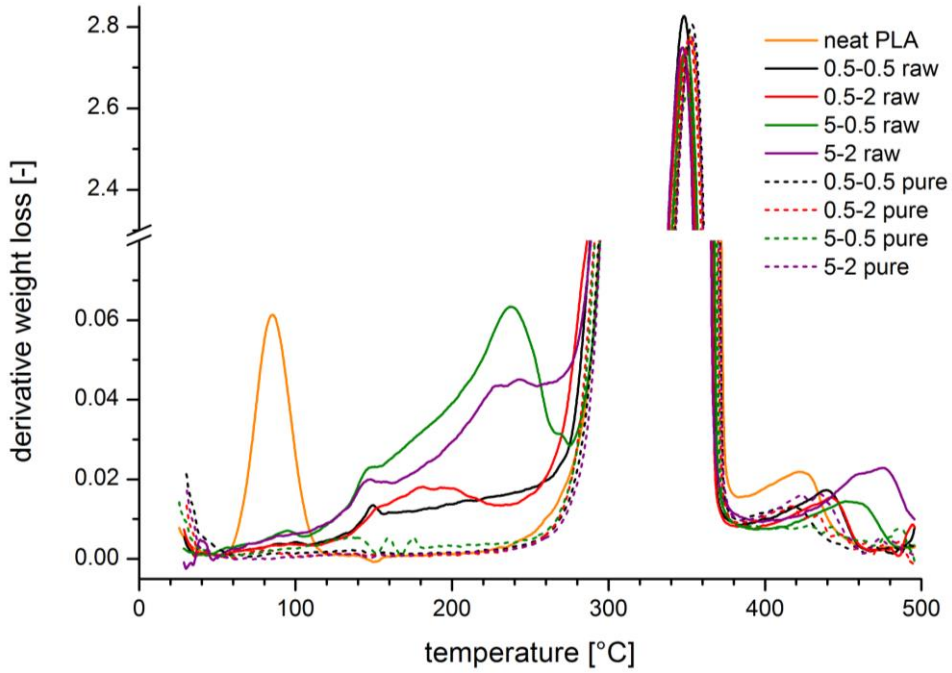

Figure 23. Derivative TGA thermograms of raw and purified PLA-g-IAH samples prepared at different $[IAH]_0$ and $[L101]_0$.

Compared to raw PLA-g-IAH, purified PLA-g-IAH contained only one decomposition step reflecting decomposition of PLA matrix. Regarding TGA thermograms in Figure 23 it is clear that both unreacted IAH and p(IAH) were succesfully removed by one-step purification.

Raw samples of PLA-g-IAH contain different byproducts detected according their different thermal stability. It is clear for PLA-g-IAH prepared with 0.5 and 5 wt % IAH. For samples 0.5-x weight loss due to water release, decomposition of unreacted IAH and residual lactide was observed whereas thermal stability of possible residues is shown in Figure 23c. On the other hand, TGA curves of samples 5-x contain derivative maxima assigned to decomposition of

unreacted IAH, residual lactide and IAH oligomers. As discussed in chapter 5.5.3, thermal decomposition consists of two distinct decomposition steps attributed to degradation of IAH and its dimers or oligomers which can be formed even without initiator (Figure 16, black curve).

6. CONCLUSION

Functionalization of PLA with IAH was achieved by post-polymerization grafting technique performed in the melt by using discontinuous mixer. This method is generally considered as one of the most practical solvent-free method which can be applied for large-scale polymers including PLA.

Reaction temperature 190 °C was calculated according to Arrhenius equation for the reaction time 6 min. This temperature is convenient for radical grafting since: a) L101 was consumed in 5 min which was proved by calculation; b) melting temperature of PLA is at least 30 °C below proposed reaction temperature which allows complete melting; c) non-radical degradation of PLA is limited at temperature below 200 °C. Under these conditions, IAH was successfuly grafted onto PLA backbone which was proved by FTIR analysis. Since C=O groups of PLA exhibit strong absorption band which overlaps C=O vibrations of grafted moieties, peak normalization method proved increased integral area of absorption band centered at 1760 cm^{-1}. In addition, C=O vibrations characteristic for IAH (1780 and 1850 cm^{-1}) were distinguished in PLA/IAH blends with amount of IAH above 1 wt % which is higher than maximum grafting degree obtained. Grafted IAH was also detected by ^{1}H-NMR spectroscopy whereas chemical shift typical for IAH oligomers was not observed.

With regard to quantitative analysis, relationship between concentration of reactants and grafting yield was determined. Low $[IAH]_0$ and $[L101]_0$ resulted in relatively high reaction conversion and low extent of undesired reactions. On the other hand, high concentration of reactants increased both grafting degree and probability of side reactions while reaction conversion was too low. After 6 min of reaction period, reaction conversion did not increase when optimized reaction conditions were applied. At low reaction temperature, low concentration of primary radicals results in higher $k_g/k_t^{1/2}$ and low both initial grafting rate and reaction conversion. At high reaction temperature, recombination of primary radicals is favoured which causes lower $k_g/k_t^{1/2}$, higher initial grafting rate and termination of grafting within short reaction period.

Despite of presumption of many researchers, polymerization of IAH was observed under conditions used for grafting. Radical polymerization of IAH in the presence of L101 was simulated whereas p(IAH) was formed at different polymerization yield depending on IAH/L101 molar ratio. It was found that low IAH/L101 molar ratio relates to higher polymerization yield because of inhibition effect of allylic hydrogen located in IAH structure. IAH polymerization was also detected in the presence of PLA during grafting reaction. High $[IAH]_0$ and $[L101]_0$ allows higher extent of IAH-L101 interactions resulting in formation of p(IAH). Possibility of IAH polymerization was considered regarding enhanced thermal stability of acetone-soluble fractions and enhanced yellowness of PLA-g-IAH samples. Except of radical polymerization of IAH, self-induced polymerization was observed using DSC and DTA. The extent of self-induced polymerization was determined to be low due to simultaneous degradation and isomerization of IAH.

Modification of PLA with IAH influenced structure of prepared PLA-g-IAH. Decrease of T_g suggests higher mobility of PLA-g-IAH chains and higher content of free volume compared to neat PLA due to bulky anhydride ring. Decrease of T_{cc} reflects decrease of molecular weight

which in consistence with results obtained from SEC. Decrease of crystallinity and grafted IAH relates to enhanced biodegradability of PLA-g-IAH compared to neat PLA.

Except of radical chain scission, non-radical degradation of PLA was evidenced. Hydrolytic degradation was suppressed by addition of chain extender Joncryl ADR-4368 C. It was predicted that reactive functional groups of chain extender reacted with both end –COOH groups of PLA and –COOH groups of IAH. Function of chain extender was identified by change of melt behavior reflecting increase of molecular weight.

PLA modified with IAH can be used for seubsequent reactions with compounds reactive towards anhydride group. PLA-g-IAH with reactive anhydride group may act as polymer substrate for "grafting through" or undergo coupling during compatibilization of polymer blends or composite materials (see Figure 1, chapter 2.1). Potential of IAH polymerization in melt could be also interesting topic for further investigation of preparation rigid p(IAH) with enhanced thermal stability and high reactivity.

7. REFERENCES

[1] Fink, J. K.: *Reactive polymers: Fundamentals and applications – A concise guide to industrial polymers*. New York: William Andrew, Inc., 2005. 770 s. ISBN 0-8155-1515-4.

[2] Moad, G.: *The synthesis of polyolefin graft copolymers by reactive extrusion*. Progress in polymer science. 1999, vol. 24, no. 1, pp. 81–142. doi:10.1016/S0079-6700(98)00017-3.

[3] Bhattacharya, A.; Misra, B. N.: *Grafting: a versatile means to modify polymers. Techniques, factors and applications*. Prog. Polym. Sci. 2004, vol. 29, no. 8, pp. 767–814. doi:10.1016/j.progpolymsci.2004.05.002.

[4] Cobo, I., Li, M., Sumerlin, B.S., Perrier, S.: *Smart hybrid materials by conjugation of responsive polymers to biomacromolecules*. Nature Materials. 2015, vol. 14, no. 2, pp. 143–159. DOI: 10.1038/nmat4106.

[5] Bhattacharya, A., Ray, P.: *Polymer grafting and crosslinking*. New Jersey: John Wiley & Sons, Inc., 2009. 341 s. ISBN 978-0-470-40465-2.

[6] Xanthos, M.: *Reactive extrusion: Principles and practice*. Hanser, Mnichov, 1992, 1st edition.

[7] Lambla, M.: *Reractive extrusion: A new tool for the diversification of polymeric materials*. Macromolecular Symposia. 1994, vol. 83, no. 1, pp. 37–48. doi: 10.1002/masy.19940830107

[8] Antonovskii, V. L.: *Initiating and cross-linking ability of organic peroxides: Chemical kinetic methods for the determination. Kinetics and catalysis*. 2003, vol. 44, no. 1, pp. 54–73. doi: 10.1023/A:1022568601041

[9] Al-Malaika, S.: *Reactive modifiers for polymers*. London: Blackie Academic & Professional, 1997. 400 s. ISBN 0-7514-0265-6.

[10] Denisov, E. T., Denisova, T. G., Pokidova, T. S.: *Handbook of free radical initiators*. New Jersey: John Wiley & Sons, Inc., 2003, 879 s. ISBN 0-471-20753-5.

[11] Berzin, F., Vergnes, B.: *Modeling of peroxide initiated controlled degradation of polypropylene in twin screw extruder*. Polymer engineering and science. 2000, vol. 40, no. 2. pp. 344–356. doi: 10.1002/pen.11168.

[12] Akbar, S., Beyou, E., Cassagnau, P., Chaumont, P., Farzi, G.: *Radical grafting of polyethylene onto MWCNTs: A model compound approach*. Polymer. 2009, vol. 50, no. 12, pp. 2535–2543. doi: 10.1016/j.polymer.2009.03.056.

[13] Lamb, D., Anstey, J.F., Fellows, C.M., Monteiro, J.M., Gilbert, R.G.: *Modification of natural and artificial polymer colloids by "topology-controlled" emulsion polymerization*. Biomacromolecules. 2001, vol. 2, no. 2, pp. 518–525. DOI: 10.1021/bm005654e.

[14] Seakins, P.W., Pilling, M.J., Niiranen, J.T., Gutman, D., Krasnoperov, L.N.: Kinetics and thermochemlstry of R + HBr ↔ RH + Br reactions: determinations of the heat of formation of C_2H_5, i-C_3H_7, sec-C_4H_9, and t-C_4H_9. Journal of polymer chemistry. 1992. vol. 96, no. 24. pp. 9847–9855. doi: 10.1021/j100203a050

[15] Bhattacharyya, S. N., Maltas, D.: *Graft copolymerization onto cellulosis*. Progress in polymer science. 1984, vol. 10, issues 2–3, pp. 171–270. doi:10.1016/0079-6700(84)90002-9.

[16] Russell, G.T., Gilbert, R.G. and Napper, D.H.: *Chain-length-dependent termination rate processes in free-radical polymerizations. 1. Theory*. Macromolecules. 1992, vol. 25, no. 9, pp. 2459–2469. DOI: 10.1021/ma00035a026.

[17] Heuts, J.P.A., Russell, G.T., Smith, G.B., Herk, A.M.: *The Importance of Chain-Length Dependent Kinetics in Free-Radical Polymerization: A Preliminary Guide*. Macromolecular Symposia. 2007, vol. 248, no. 1, pp. 12–22. DOI: 10.1002/masy.200750202.

[18] Gilbert, R.G.: *Emulsion polymerization: A mechanistic approach*. Polymer. 1997, vol. 38, no. 10, pp. 2577–2578. doi:10.1016/S0032-3861(96)01078-6.

[19] Garlotta, D.: *A literature review of poly(lactic acid)*. Journal of polymers and the environment. 2002, vol. 9, no. 2, pp. 63–84. DOI: 10.1023/A:1020200822435.

[20] Mani, R., Bhattacharya, M., Tang, J.: *Functionalization of polyesters with maleic anhydride by reactive extrusion*. Journal of polymer science: Part A: Polymer chemistry. 1999, vol. 37, no. 11, pp. 1693–1702. DOI: 10.1002/(SICI)1099-0518(19990601)37:11<1693::AID-POLA15>3.0.CO;2-Y.

[21] Carlson, D., Dubois, P., Nie, L.,Narayan, R.: *Free radical branching of polylactide by reactive extrusion*. Polymer engineering and science. 1998, vol. 38, no. 2, pp. 311–321. DOI: 10.1002/pen.10192.

[22] Ramkumar, D.H.S., Bhattacharya, M., Vaidya, U.R.: *Properties of injection moulded starch/synthetic polymer blends - II. Evaluation of mechanical properties*. European Polymer Journal. 1997, vol. 33, no. 5, pp. 729–742. doi:10.1016/S0014-3057(96)00216-9.

[23] John, J., Tang, J., Yang, Z., Bhattacharya, M.: *Synthesis and characterization of anhydride-functional polycaprolactone*. Journal of Polymer Science Part A: Polymer Chemistry. 1997, vol. 35, no. 6, pp. 1139–1148. DOI: 10.1002/(SICI)1099-0518(19970430)35:6<1139::AID-POLA17>3.0.CO;2-7.

[24] Mani, R., Bhattacharya, M.: *Properties of injection moulded blends of starch and modified biodegradable polyesters*. European Polymer Journal. 2001, vol. 37, no. 3, pp. 515–526. doi:10.1016/S0014-3057(00)00155-5.

[25] Pan, J.; Wang, Y., Qin, S., Zhang, B., Luo, Y.: *Grafting reaction of poly($_{D,L}$)lactic acid with maleic anhydride and hexanediamine to introdukce more reactive groupy in its bulk.* Applied biomaterials. 2005, vol. 74, no. 1, pp. 476–480. DOI: 10.1002/jbm.b.30208.

[26] Carlson, D., Nie, L., Narayan, R., Dubois, P.: *Maleation of polylactide (PLA) by reactive extrusion*. Journal of applied polymer science. 1999, vol. 72, no. 4, pp. 477–485. DOI: 10.1002/(SICI)1097-4628(19990425)72:4<477::AID-APP3>3.0.CO;2-Q.

[27] Hwang, S. W., Lee, S.B., Lee, Ch.K., Lee, J.Y., Shim, J.K., Selke, S.E.M., Soto-Valdez, H., Matuana, L., Rubino, M., Auras, R.: *Grafting of Maleic Anhydride on Poly(L-lactic acid): Effects on Physical and Mechanical Properties*. Polymer Testing. 2012, vol. 31, no. 2, pp. 333–344. doi:10.1016/j.polymertesting.2011.12.005.

[28] Plackett, D.: *Maleated polylactide as an interfacial compatibilizer in biocomposites*. Journal of polymers and the environment. 2004, vol. 12, no. 3, pp. 131–138. DOI: 10.1023/B:JOOE.0000038544.75554.0e.

[29] Zhang, J. F., Sun, X.: *Mechanical properties of poly(lactic acid)/starch composites compatibilized by maleic anhydride*. Biomacomolecules. 2004, vol. 5, no. 4, pp. 1446–1451. DOI: 10.1021/bm0400022.

[30] Rezgui, F., G'Sell, C., Dahoun, A., Hiver, J.M., Sadoun, T.: *Plastic deformation of low-density polyethylene reinforced with biodegradable , part 1: Microstructural analysis and tensile behavior at konstant true strain-rate*. Polymer engineering and science. 2011, vol. 51, no. 1, pp. 117–125. DOI: 10.1002/pen.21797.

[31] Reddy, N., Nama, D., Yang, Y.: *Polylactic acid/polypropylene polyblend fibres for better resistence to degradation*. Polymer Degradation and Stability. 2008, vol. 93, no. 1, pp. 233–241. doi:10.1016/j.polymdegradstab.2007.09.005.

[32] Singh, G., Bhunia, H., Rajor, A., Jana, R.N., Choudhary, V.: *Mechanical properties and morfology of polylactide, linear low-density polyetylene and their blends*. Journal of applied polymer science. 2010, vol. 118, no. 1, pp. 496–502. DOI: 10.1002/app.32305.

[33] Smedberg, A., Hjertberg, T., Gustaffson, B.: *Crosslinking reactions in an unsaturated low density polyethylene*. Polymer. 1997, vol. 38, no. 16, pp. 4127–4138. doi:10.1016/S0032-3861(96)00994-9.

[34] Clark, D.C., Baker, W.E., Whitney, R.A.: *Peroxide-initiated comonomer grafting of styrene and maleic anhydride onto polyethylene: Effect of polyethylene microstructure*. Journal of Applied Polymer Science. 2001, vol. 79, no. 1, pp. 96–107. DOI: 10.1002/1097-4628(20010103)79:1<96::AID-APP120>3.0.CO;2-X.

[35] Tyuganova, M.A., Galbraikh, L.S., Ulmasove, A.A., Tsarevskaya, I.Y., Khidoyator, A.A.: *Use of rice straw as cellulosic raw material for ion exchanger production*. Cellulose Chemistry and Technology. 1985, vol. 19, no. 5, pp. 557–568.

[36] Roover, B. D., Sclavons, M., Carlier, V., Devaux, J., Legras, R., Momtaz, A.: *Molecular characterization of maleic anhydride-functionalized polypropylene*. Journal of polymer science: Part A: Polymer chemistry. 1995, vol. 33, no. 5, pp. 829–842. DOI: 10.1002/pola.1995.080330509.

[37] De Roover, B., Devaux, J., Legras, R.: *Maleic anhydride homopolymerization during melt functionalization of isotactic polypropylene*. Journal of polymer science: Part A: Polymer chemistry. 1996, vol. 34, no. 7, pp. 1195–1202. DOI: 10.1002/(SICI)1099-0518(199605)34:7<1195::AID-POLA5>3.0.CO;2-2.

[38] Bettini, S. H. P., Agnelli, J. A. M.: *Grafting of maleic anhydride onto polypropylene by reactive processing. I. Effect of maleic anhydride and peroxide concentrations on the reaction*. Journal of applied polymer science. 1999, vol. 74, no. 2, pp. 247–255. DOI: 10.1002/(SICI)1097-4628(19991010)74:2<247::AID-APP2>3.0.CO;2-A.

[39] Yokota, K., Hirabayashi, T., Takashima, T.: *Preparation of poly(itaconic acid)*. Die Makromolekulare Chemie. 1975, vol. 176, no. 5, pp. 1197–1205. doi: 10.1002/macp.1975.021760501.

[40] Atofina Chemical Inc. Organic Peroxides. U.S.A: Technical Data. 2001.

[41] Karst, D., Yang, Y.: *Using the solubility parameter to explain disperse dye sorption on polylactide*. Journal of Applied Polymer Science. 2000, vol. 96, no. 2, pp. 416–422. DOI: 10.1002/app.21456.

[42] Fukuoka, T.: *Numerical analysis of a reactive extrusion process. Part I: Kinetics study on grafting of vinylsilane to polyethylene*. Polymer Engineering and Science 2000, vol. 40, no. 12, pp. 2511–2523. DOI: 10.1002/pen.11382.

[43] Heinen, W., Rosenmöller, C.H., Wenzel, C.B., de Groot, H.J.M., Lugtenburg, J., van Duin, M.: *^{13}C NMR Study of the Grafting of Maleic Anhydride onto Polyethene, Polypropene, and Ethene−Propene Copolymers*. Macromolecules. 1996, vol. 29, no. 4, pp. 1151–1157. DOI: 10.1021/ma951015y.

[44] Russell, K.E., Kelusky, E.C.: *Grafting of maleic anhydride to n-eicosane*. Journal of Polymer Science Part A: Polymer Chemistry. 1988, vol. 26, no. 8, pp. 2273–2280. DOI: 10.1002/pola.1988.080260821.

[45] Rice, F.O., Murphy, M.T.: The Thermal Decomposition of Five-Membered Rings. Journal of the american chemical society. 1942, vol. 64, no. 4, pp. 896–899. DOI: 10.1021/ja01256a046.

[46] Otsu, T., Yang, J-Z.: *Radical polymerization of itaconic anhydride and reactions of the resulting polymers with amines and alcohols*. Polymer international. 1991, vol. 25, no. 4, pp. 245–251. DOI: 10.1002/pi.4990250408.

[47] Katime, I., Madoz, A., Velada, J. L.: *The kinetics of bulk polymerization of itaconate derivates. Part 2. Diphenyl, dibenzyl and di-2-phenylethyl itaconates*. Thermochim. Acta. 1993, vol. 220, pp. 91–101. DOI: 10.1016/0040-6031(93)80457-L.

[48] Milovanovic, M.B., Trifunovic, S., Katsikas, L., Popovic, I.G.: Preparation and modification of itaconic anhydride-methyl methacrylate copolymers. Journal of the Serbian chemical society. 2007, vol. 72, no. 12, pp. 1507–1514. doi:10.2298/JSC0712507M.

[49] Velada, J.L., Hernáez, E., Cesteros, L.C., Katime, I.: A study of the thermal degradation of several poly(monoalkylaryl itaconates). Polymer Degrdation and Stability. 1996, vol. 52, no. 3, pp. 273–282. doi:10.1016/0141-3910(96)00008-0.

[50] Shang, S., Huang, S.J., Weiss, R.A.: *Synthesis and characterization of itaconic anhydride and stearyl methacrylate copolymers*. Polymer. 2009, vol. 50, no. 14, pp. 3119–3127. doi:10.1016/j.polymer.2009.05.012.

[51] Ishida S, Saito S.: Polymerization of itaconic acid derivatives. Journal of Polymer Science, Part A-1: Polymer Chemistry. 1967, vol. 5, no. 4, pp. 689–705. DOI: 10.1002/pol.1967.150050401.

[52] Nagai, S.: The polymerization and polymer sof itaconic acid derivates. VI. The polymerization and copolymerization of itaconic anhydride. 1964, vol. 37, no. 3, pp. 369–373. DOI: 10.1246/bcsj.37.36.

[53] Luo, Y., Wang, Y., Niu, X., Fu, Ch., Wang, S.: *Synthesis, characterization and biodegradation of butanediamine-grafted poly($_{DL}$-lactic acid)*. European polymer journal. 2007, vol. 43, no. 9, pp. 3856–3864. doi:10.1016/j.eurpolymj.2007.06.022.

[54] Wu, X. S., Wang, N.: *Synthesis, characterization, biodegradation and drug delivery application of biodegradable lactic/glycolic acid polymers. Part II: Biodegradation.* Journal of biomaterial science polymer edition. 2001, vol. 12, no. 1, pp. 21–34. DOI:10.1163/156856201744425.

[55] Tábi, T., Sajó, I.E., Szabó, F., Luyt, A.S., Kovács, J.G.: *Crystalline structure of annealed polylactic acid and its relation to processing*. eXPRESS polymer letters. 2010, vol. 4, no. 10, pp. 659–668. DOI: 10.3144/expresspolymlett.2010.80.

[56] Fakirov, S.: Biodegradable polyesters. John Wiley & Sons, 2015. ISBN 3527330860.

[57] Fischer, E. W., Sterzel, H. J., Wenger, G.: *Investigation of the structure of solution grown crystals of lactide copolymers by means of chemical reactions*. Kolloid-Zeitschrift und Zeitschrift für Polymere. 1973. vol. 251, no. 11, pp. 980–990. DOI: 10.1007/BF01498927.

LIST OF ABBREVIATIONS

PLA	poly(lactic acid)
IAH	itaconic anhydride
L101	2,5-bis(tert-butylperoxy)-2,5-dimethylhexane
PLA-g-IAH	poly(lactic acid) grafted with itaconic anhydride
$[IAH]_{PLA}$	grafting degree
$[IAH]_0$	initial concentration of itaconic anhydride
$[L101]_0$	initial concentration of initiator 2,5-bis(tert-butylperoxy)-2,5-dimethylhexane
$PLA^{\bullet}$	PLA macroradical
$IAH^{\bullet}$	IAH radical
$L101^{\bullet}$	radical species generated via thermal decomposition of initiator
$\tau_{1/2}$	half-life time of peroxide initiator
T_g	glass transition temperature
T_{cc}	cold crystallization temperature
T_m	melting temperature
X_c	degree of crystallinity
T_{max}	maximum decomposition rate temperature
k_i	initiation rate constant
k_p	propagation rate constant
k_t	termination rate constant
E_a	activation energy
E_d	dissociation energy
δ	solubility parameter
T_c	ceiling polymerization temperature
ΔH_p	polymerization enthalpy
ΔS_p	polymerization entropy
ΔH_r	heat of reaction
FTIR	Fourier transform infrared spectroscopy
ATR	attenuated total reflection measurement mode
DSC	differential scanning calorimetry
TGA	thermogravimetric analysis
DTA	differential thermal analysis
SEC	size exclusion chromatography
^{1}H-NMR	proton nuclear magnetic resonance
MFR	melt flow rate
PLA-g-MAH	poly(lactic acid) grafted with maleic anhydride
p(IAH)	poly(itaconic anhydride)
DBP	dibenzoyl peroxide
TBP	tert-butyl peroxide
$CDCl_3$	deuterated chloroform
KOH	potassium hydroxide
THF	tetrahydrofuran

LIST OF FIGURES

LIST OF TABLES